ANALYSIS OF EVAPORATIVE LAKES IN NHECOLANDIA, PANTANAL BASIN, BRAZIL

Taquari megafan, Pantanal

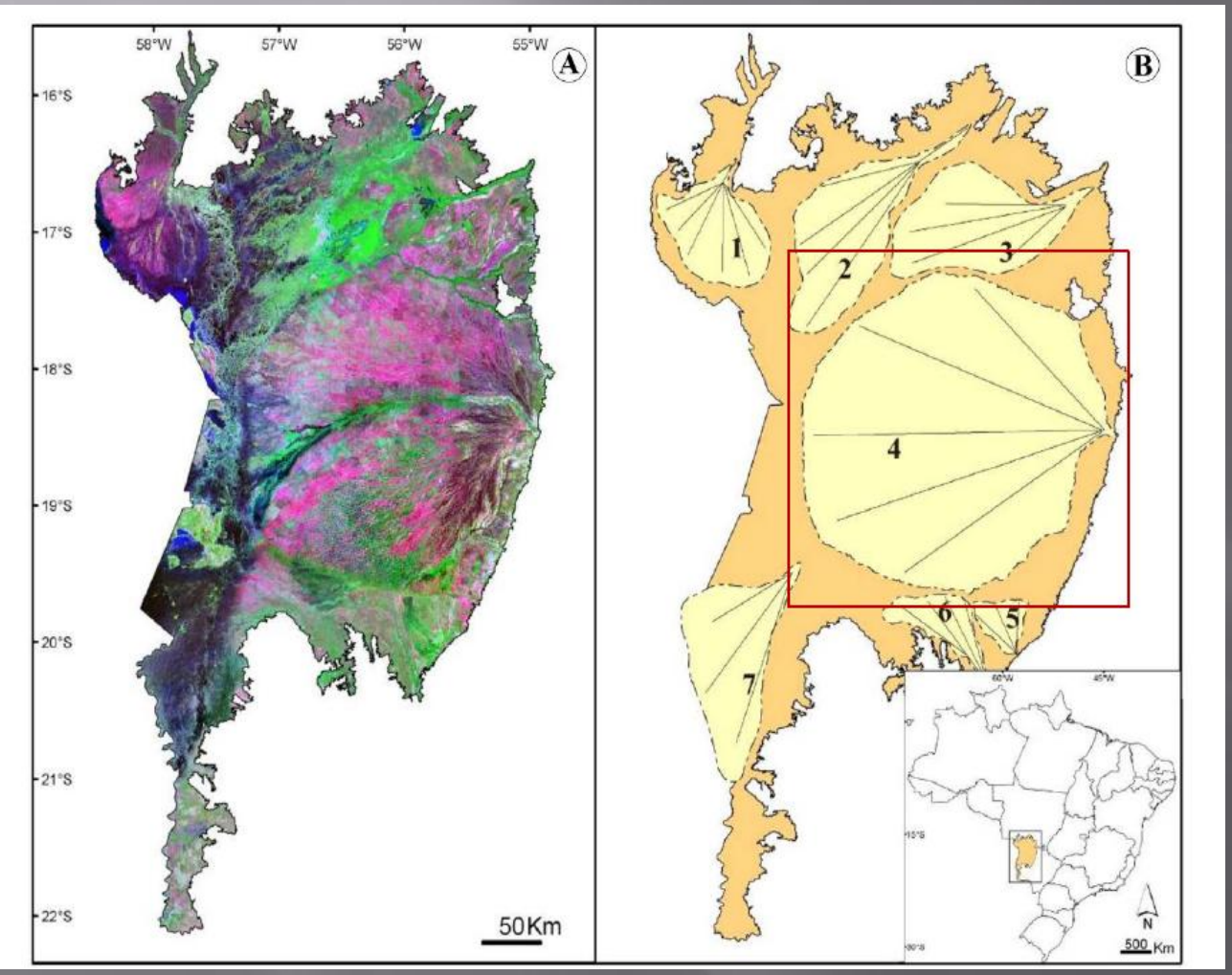

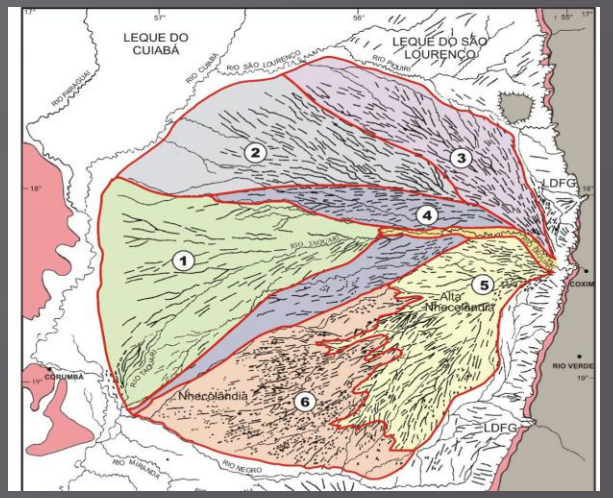

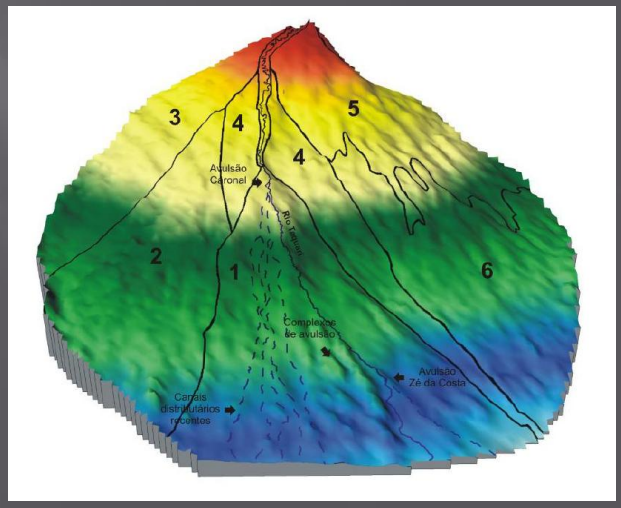

From Zani, et al. (2006)


A)
Colombia
Brazil
Peru
Bolivia
Paraguay
Argentina
Uruguay
Chile
N

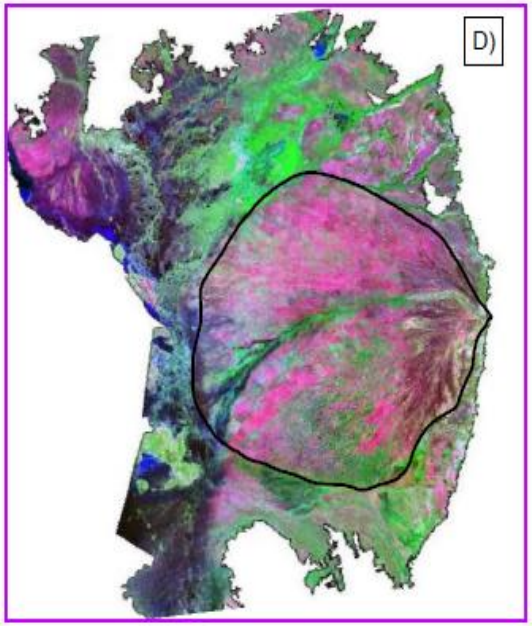
D)

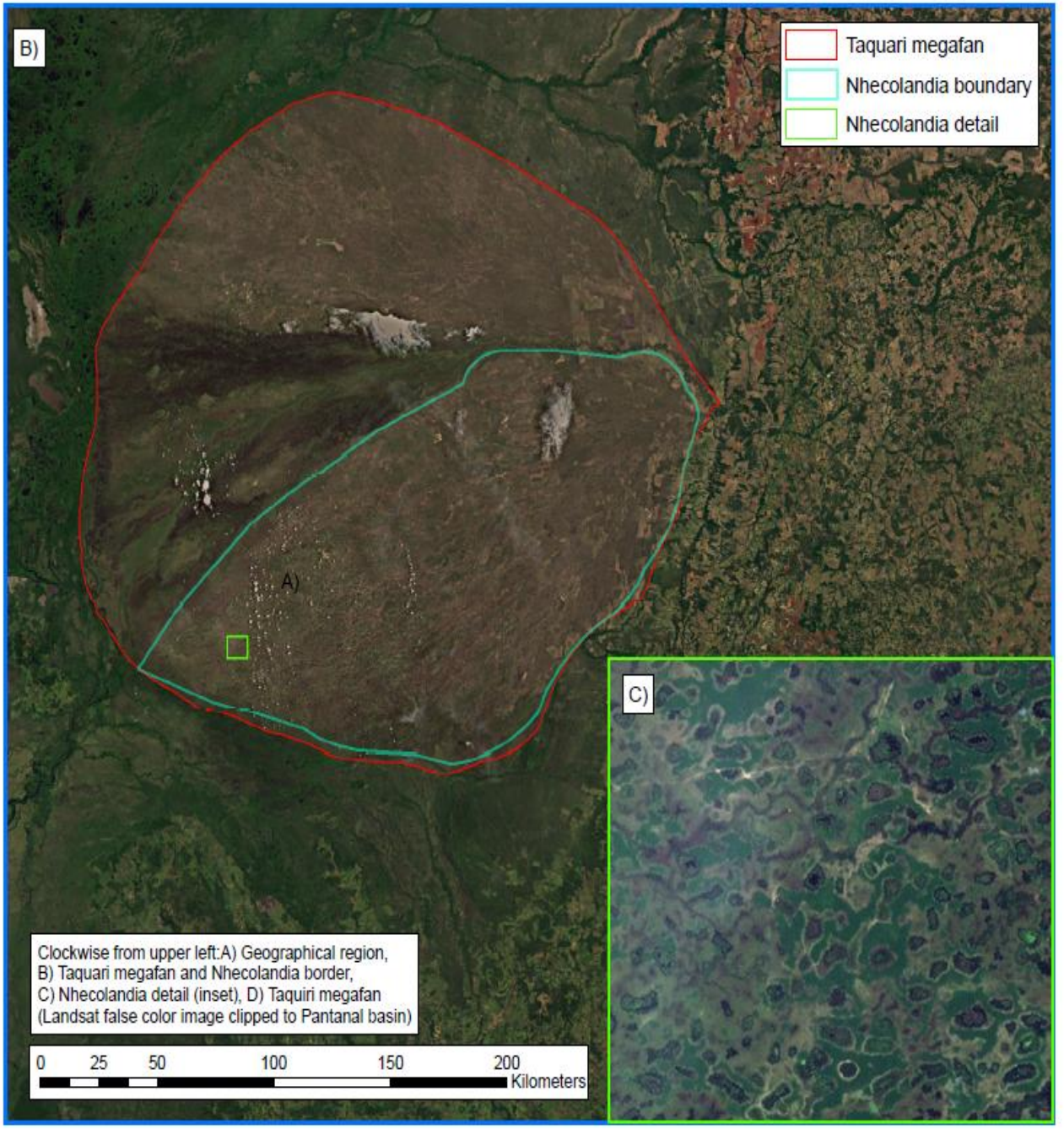
B)
Taquari megafan
Nhecolandia boundary
Nhecolandia detail
A)
C)
Clockwise from upper left:A) Geographical region,
B) Taquari megafan and Nhecolandia border,
C) Nhecolandia detail (inset), D) Taquiri megafan
(Landsat false color image clipped to Pantanal basin)
0 25 50 100 150 200
Kilometers

Process for Lake Differentiation

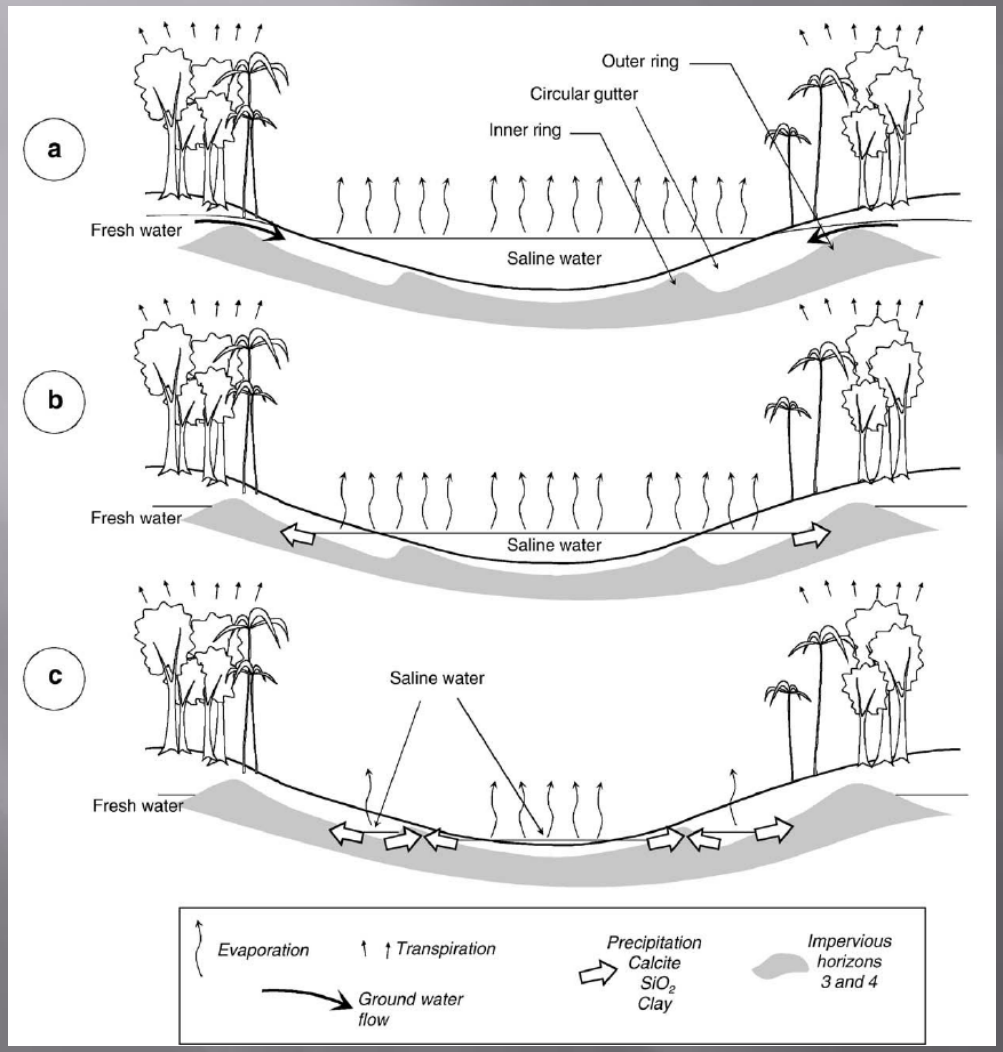

From Barbeiro et al. (2008)

- Barbeiro et al. (2002, 2008)
- Waters of all lakes in same chemical family
- Evaporative concentration process in saline lakes
- Impervious soil horizon(s) (grey) control groundwater flow in saline lakes
- (A) Wet season
- (B) Dry Season
- (C) Drought

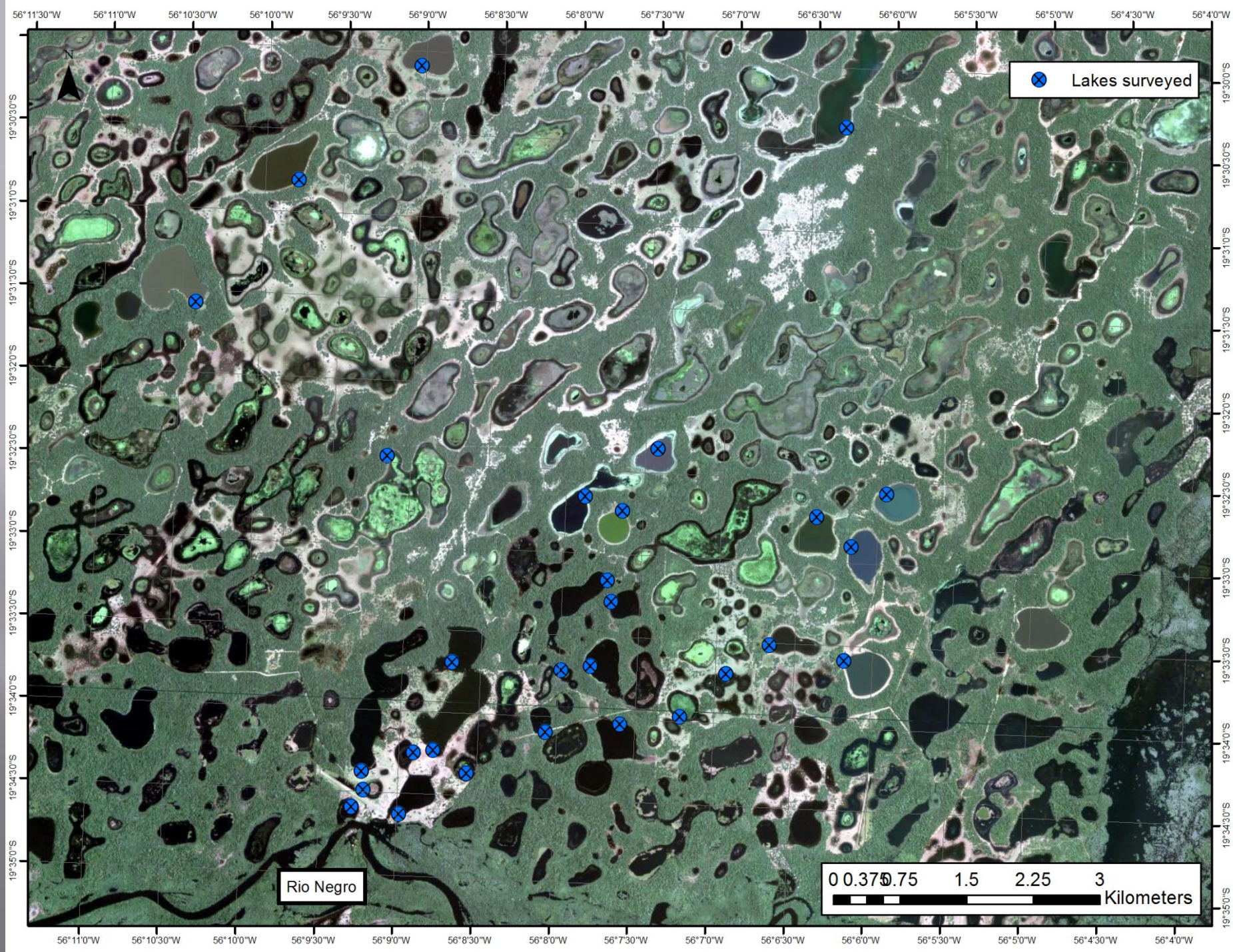
Lakes surveyed
Rio Negro
0 0.375 0.75 1.5 2.25 3
Kilometers
N
56°11'30"W
56°11'0"W
56°10'30"W
56°10'0"W
56°9'30"W
56°9'0"W
56°8'30"W
56°8'0"W
56°7'30"W
56°7'0"W
56°6'30"W
56°6'0"W
56°5'30"W
56°5'0"W
56°4'30"W
56°4'0"W
19°30'30"S
19°31'0"S
19°31'30"S
19°32'0"S
19°32'30"S
19°33'0"S
19°33'30"S
19°34'0"S
19°34'30"S
19°35'0"S

Analyses performed

- Spring/Fall 2012:
  - Water chemistry: major cations and anions
  - PhreeqC evaporation model
  - Stable isotopes of O and H
  - Initial lake budget model
  - Remote sensing classification
- Spring 2013
  - TEM analysis of geologic samples
  - Refine RS with new imagery

http://www.soboi.com.br/mostra.asp?noticias=3748&Classe=

Proposed Analysis 2013

- Off-season samples (March-June) by FBA workers

- Intensive repeat water sampling
  - Multi-level instrument
  - Data Logger?

- Calibrated evaporation pan?

- 2nd RS analysis:
  - Segmentation of postage stamp
  - Time-series flood analysis w/ new imagery source

http://www.soboi.com.br/mostra.asp?noticias=3748&Classe=

Water Chemistry Summary (Cations and Anions in ppm)

ID	Ca	Mg	Na	K	CO3	HCO3	alk as HCO3	SO4	Cl	Balance	EC	pH (field)	T ©
Rio	1.464	0.924	1.259	2.441	0	12.37425	12.3742476	0.481484	1.110273	4.71	52.5	5.58	25.5
L20	0.326	0.294	4.094	8.739	0	18.56137	18.5613714	0.520061	4.328353	1.23	74.5	6.01	25
L27	5.688	4.924	55.08	19.204	0	228.9236	228.9235806	0.320313	7.03549	-3.32	374	7.02	28.3
Wel	7.77	5.868	110.9	28.61	0	309.3562	309.35619	3.279363	61.63382	-1.22	650	6.38	26.8
L19	3.57	2.56	171.925	60.46	27.9906	555.6037	612.5179331	*3*	17.92828	-5.63	895	8.69	26.6
L10	7.807	1.378	252	80.82	60.84913	668.2094	791.9359266	13.76022	37.95213	-2.03	1299	9.12	23.6
L25	4.987	0.845	242.1	174.7	85.18878	810.5132	983.7303965	0.588634	20.7366	-3.51	1503	8.95	31.4
L11	2.53	0.24	843.2	163.92	498.9628	1076.56	2091.117302	*20*	382.3613	-3.10	3890	9.89	25.5
L29	2.51	*0.25*	963.2	179.96	669.3404	1008.501	2369.493298	22.85516	231.6018	2.49	2330	9.79	31
L22	0.59	*0.25*	1181.2	168.24	584.1516	1416.851	2604.62629	*20*	365.4459	4.53	5010	9.61	*26*
L26	*0.5*	*0.25*	3084.333	599.4667	571.9818	618.7124	1781.742008	*20*	4732.769	-3.71	16150	9.77	32

Table 1: Summary of major cations, anions, and field parameters. Color-coding indicates relative salinity (blue low to red high - green indicates anomalously Cl- rich lake L26)

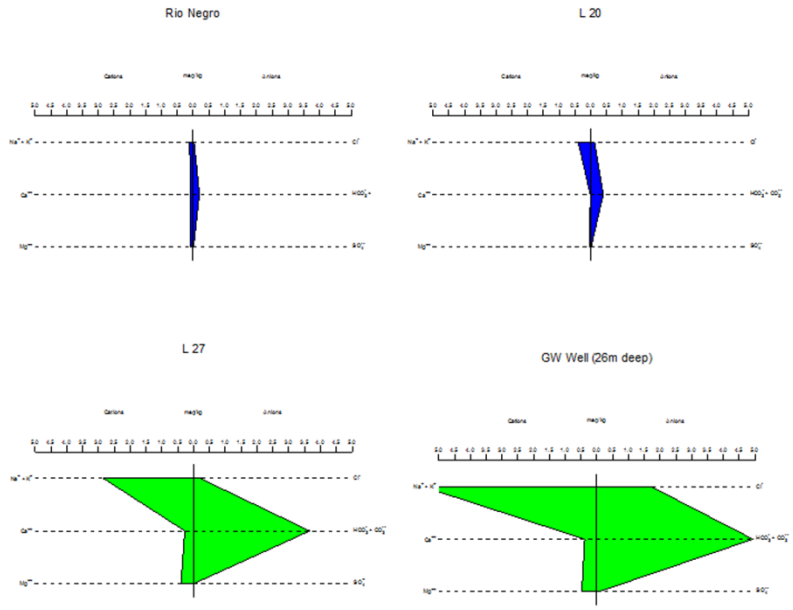

Figures 4a and b: Stiff diagrams of two "freshest" sample groups at constant meq scale.

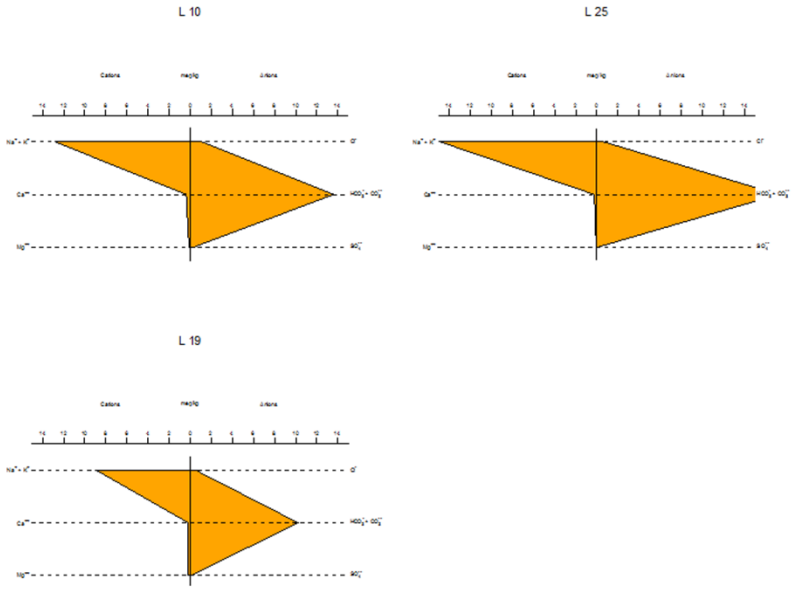

Figure 5: Stiff diagrams from mildly saline group 3, note meq scale has been increased to accomadate higher cation and anion concentrations.

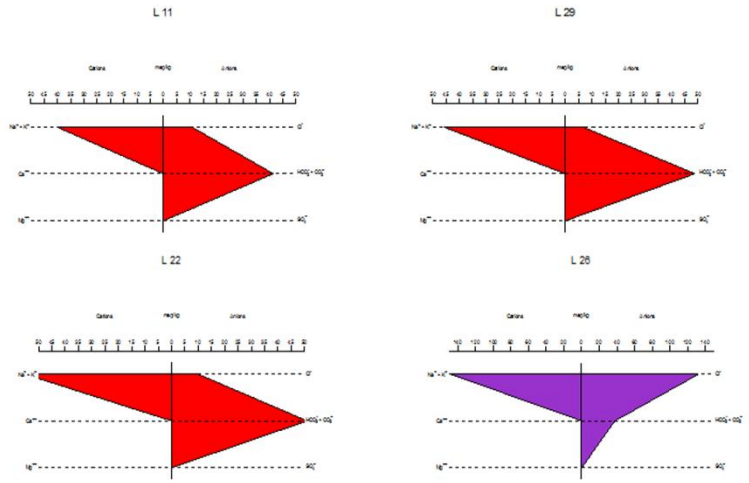

Figure 6 and 7 : Stiff diagrams for group 4 (brackish) and group 5 (saline) samples. Note scale is constant for figures in red and increased to accomodate higher salinity of L26 (purple).

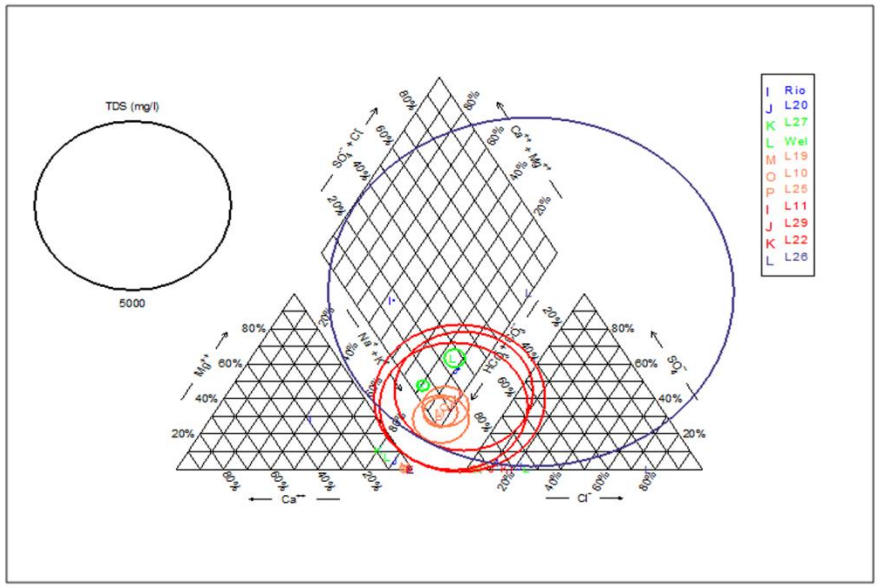

Figure 8: Piper diagram of all waters sampled. Circle diameter indicates total salinity (scale in upper left). See text for further discussion.

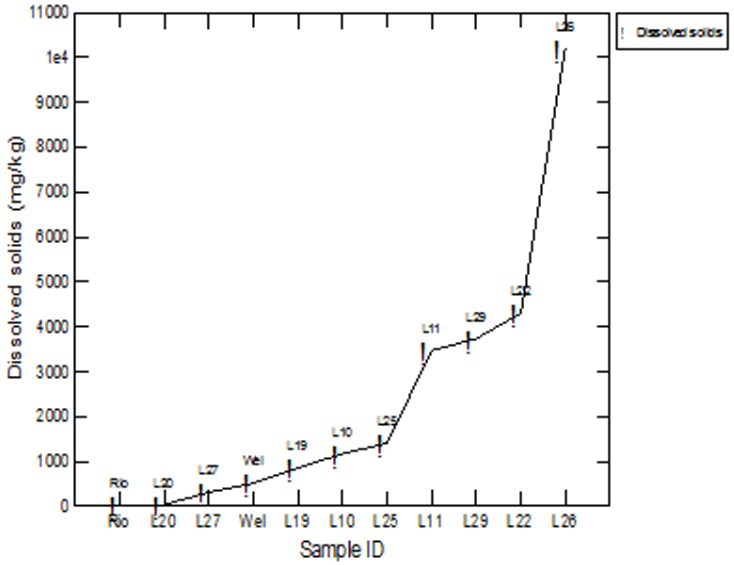

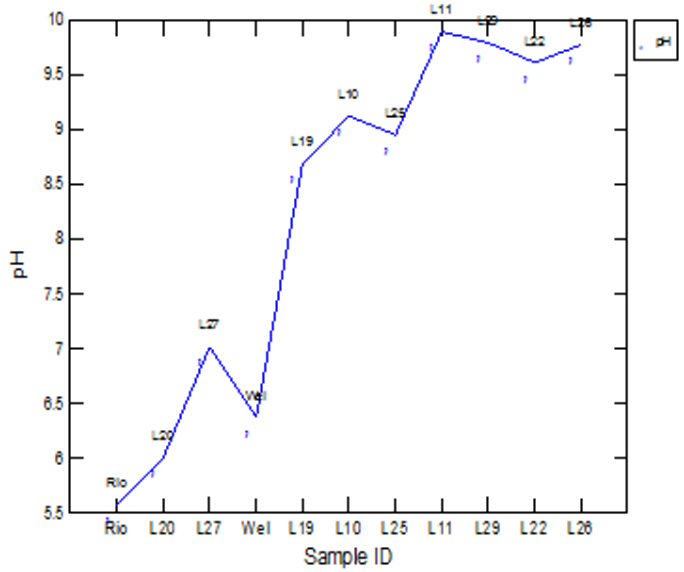

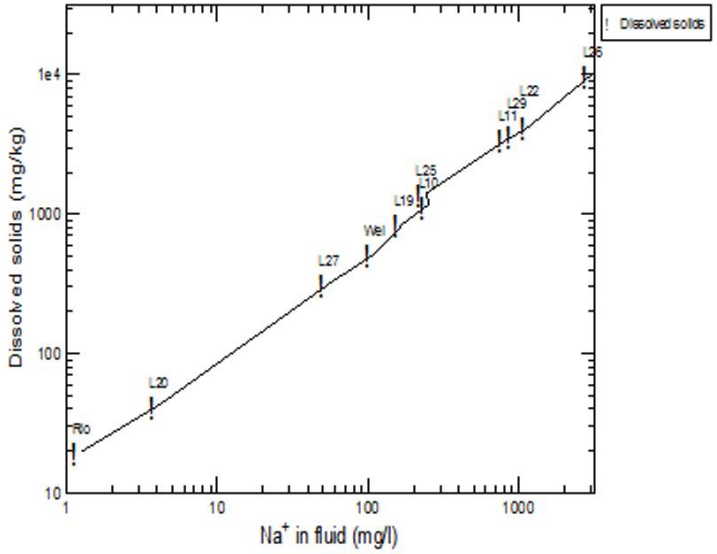

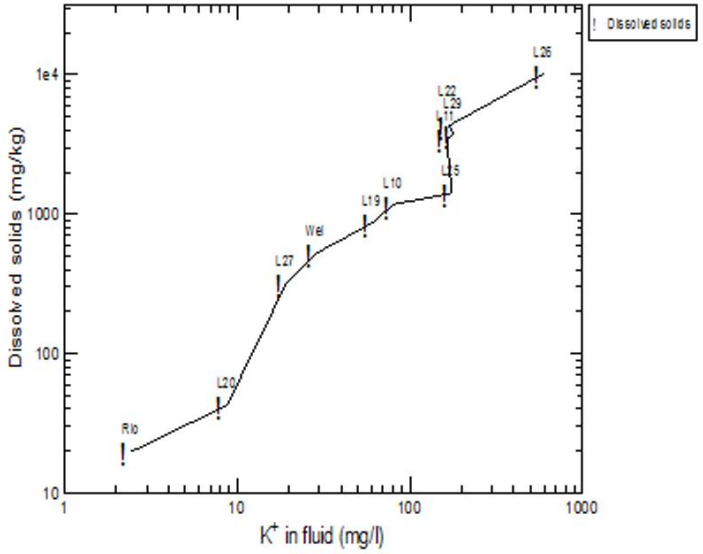

Figures 11 and 12: Na+ vs. salinity, K+ vs. salinity

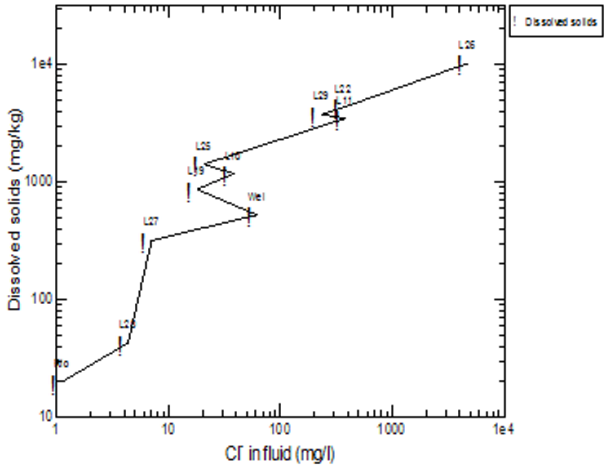

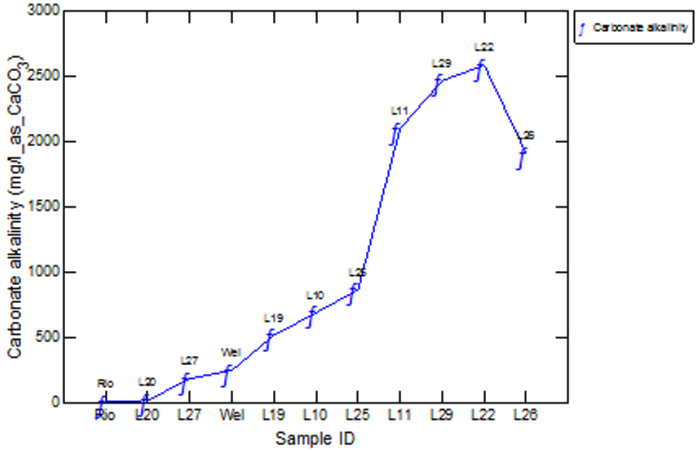

Figures 13 and 14: Chloride vs. TDS, Total alkalinity (as CaCO3) for all samples

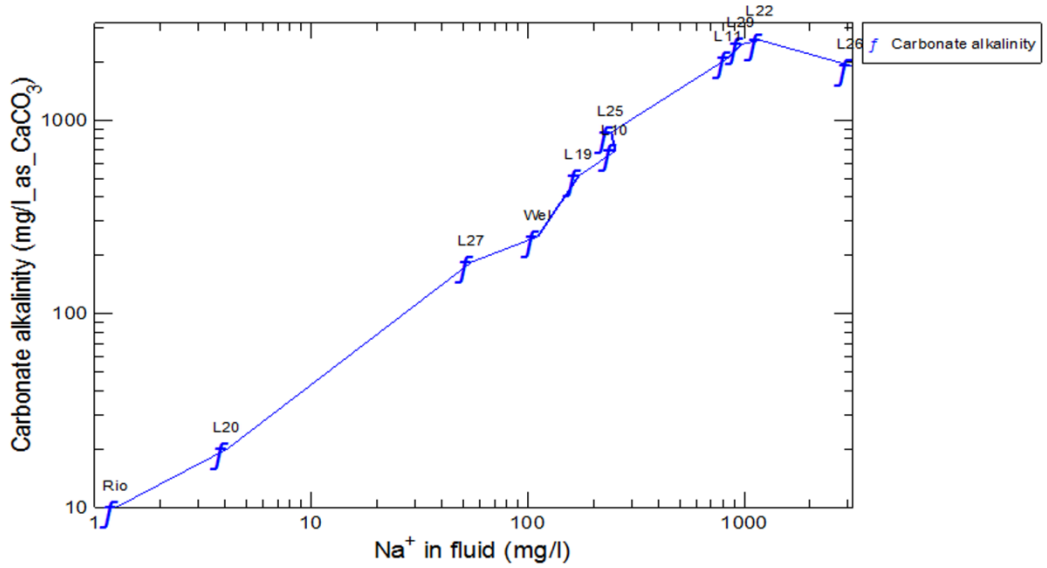

Figure 15: Na+ vs. Total alkalinity (as CaCO3)

Simple Evap. Model (95%)

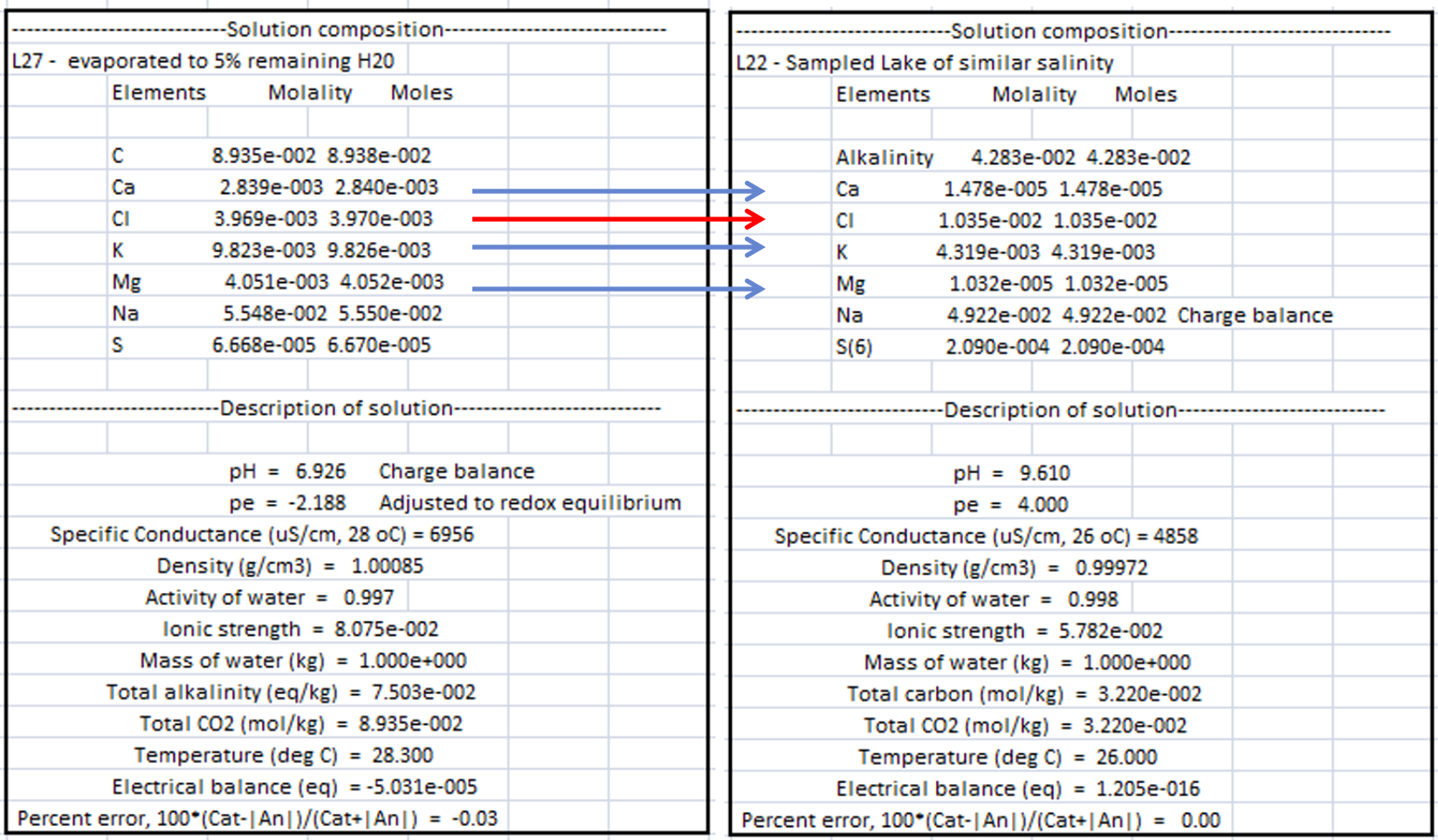

----------Solution composition----------

L27 - evaporated to 5% remaining H20

Elements	Molality	Moles
C	8.935e-002	8.938e-002
Ca	2.839e-003	2.840e-003
Cl	3.969e-003	3.970e-003
K	9.823e-003	9.826e-003
Mg	4.051e-003	4.052e-003
Na	5.548e-002	5.550e-002
S	6.668e-005	6.670e-005

----------Description of solution----------

pH = 6.926 Charge balance
pe = -2.188 Adjusted to redox equilibrium
Specific Conductance (uS/cm, 28 oC) = 6956
Density (g/cm3) = 1.00085
Activity of water = 0.997
Ionic strength = 8.075e-002
Mass of water (kg) = 1.000e+000
Total alkalinity (eq/kg) = 7.503e-002
Total CO2 (mol/kg) = 8.935e-002
Temperature (deg C) = 28.300
Electrical balance (eq) = -5.031e-005
Percent error, 100*(Cat-|An|)/(Cat+|An|) = -0.03

----------Solution composition----------

L22 - Sampled Lake of similar salinity

Elements	Molality	Moles	
Alkalinity	4.283e-002	4.283e-002	
Ca	1.478e-005	1.478e-005	
Cl	1.035e-002	1.035e-002	
K	4.319e-003	4.319e-003	
Mg	1.032e-005	1.032e-005	
Na	4.922e-002	4.922e-002	Charge balance
S(6)	2.090e-004	2.090e-004	

----------Description of solution----------

pH = 9.610
pe = 4.000
Specific Conductance (uS/cm, 26 oC) = 4858
Density (g/cm3) = 0.99972
Activity of water = 0.998
Ionic strength = 5.782e-002
Mass of water (kg) = 1.000e+000
Total carbon (mol/kg) = 3.220e-002
Total CO2 (mol/kg) = 3.220e-002
Temperature (deg C) = 26.000
Electrical balance (eq) = 1.205e-016
Percent error, 100*(Cat-|An|)/(Cat+|An|) = 0.00

Tables 2 and 3: Result of PhreeqC simple evaporation (REACTION -1 H2O stepwise until 52.8 moles H2O removed)

PhreeqC Inverse Model

Solution 1: L19				Solution 2: L11			
	Input	Delta	Input+Delta		Input	Delta	Input+Delta
Alkalinity	1.004e-002	+ 0.000e+000	= 1.004e-002	Alkalinity	3.428e-002	+ -6.183e-004	= 3.366e-002
C(4)	1.206e-002	+ -7.276e-005	= 1.198e-002	C(4)	4.051e-002	+ 0.000e+000	= 4.051e-002
Ca	8.914e-005	+ 0.000e+000	= 8.914e-005	Ca	6.332e-005	+ 0.000e+000	= 6.332e-005
Cl	5.061e-004	+ 0.000e+000	= 5.061e-004	Cl	1.082e-002	+ 0.000e+000	= 1.082e-002
K	1.547e-003	+ 0.000e+000	= 1.547e-003	K	4.205e-003	+ 1.055e-003	= 5.260e-003
Na	8.672e-003	+ 1.501e-004	= 8.822e-003	Na	4.124e-002	+ -2.144e-003	= 3.910e-002

Solution fractions:		Minimum	Maximum
Solution	1 3.400e+000	0.000e+000	0.000e+000
Solution	2 1.000e+000	0.000e+000	0.000e+000

Phase mole transfers:		Minimum	Maximum	
H2O	-1.332e+002	0.000e+000	0.000e+000	H2O
Calcite	-2.398e-004	0.000e+000	0.000e+000	CaCO3
Halite	9.099e-003	0.000e+000	0.000e+000	NaCl

Summary of inverse modeling:

Number of models found: 2
Number of minimal models found: 2
Number of infeasible sets of phases saved: 9
Number of calls to cl1: 35

Table 4: Result of PhreeqC evaporative inverse model (INVERSE MODEL L19 to L11 - only Ca+, Cl-, K+, Na+ conserved)

Stable isotope results

Analyzed $\delta^{18}O$ and $\delta^{2}H$
- Picarro isotopic analyzer
- Laser cavity ring-down spectroscope

Distillation of saline waters
- Select samples distilled
- Compared to original samples
- Accepted distillation process as valid
- No fractionation (w/ 100% distillation)

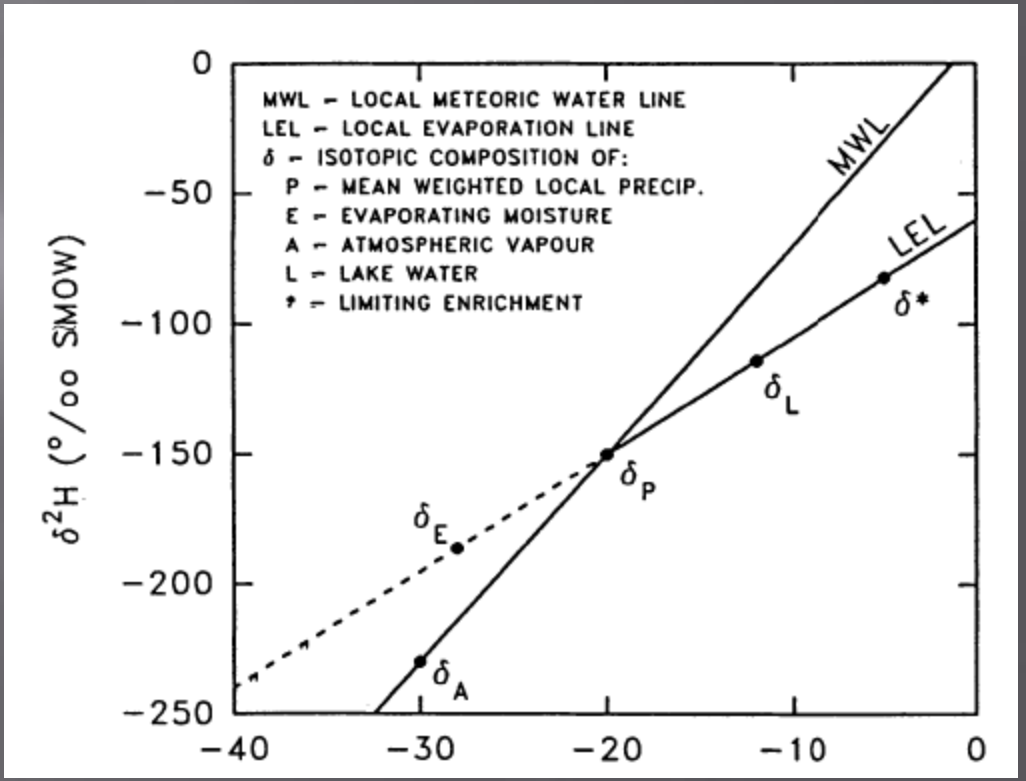

Results – all samples

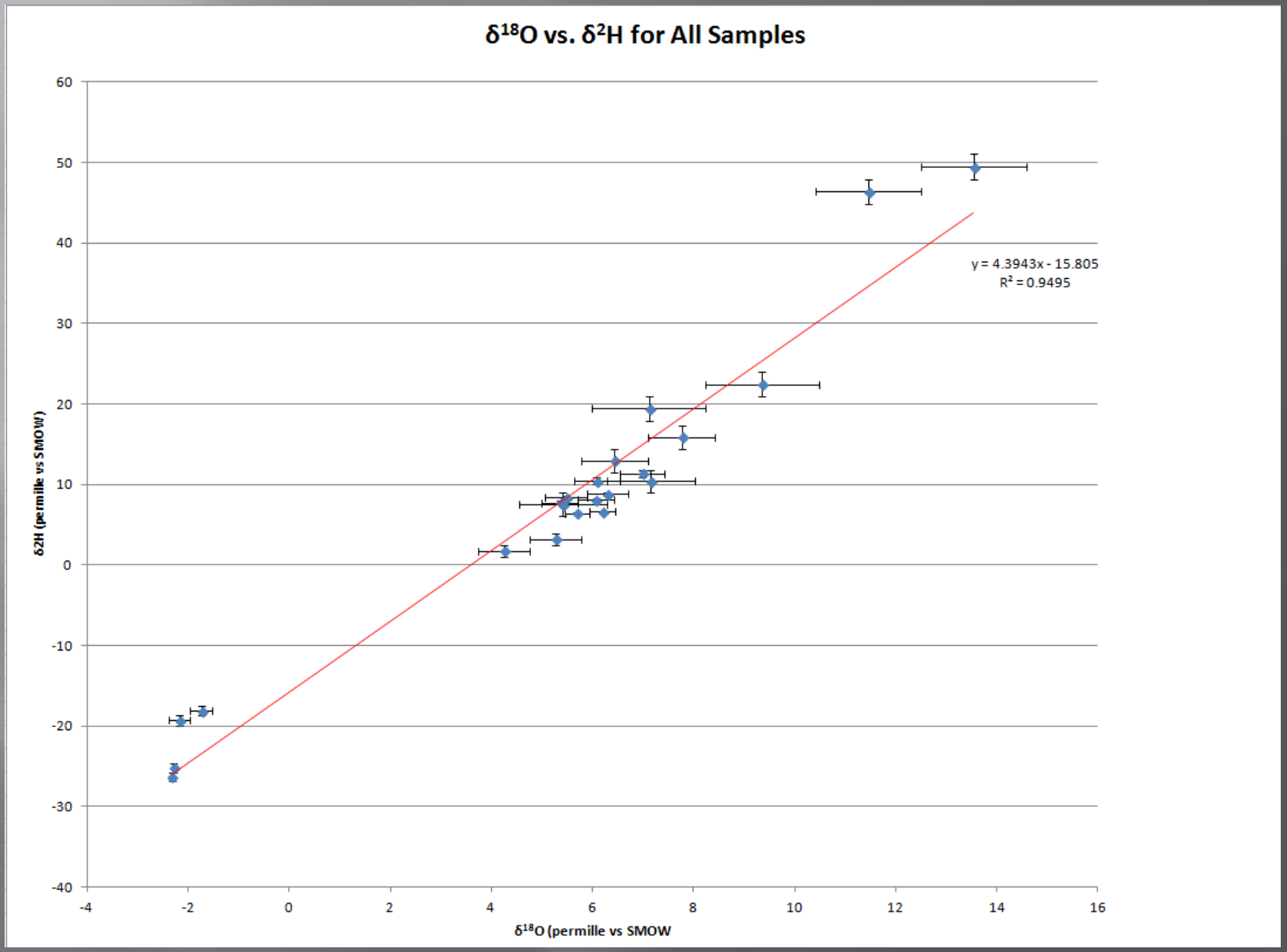

Results - Interpreted

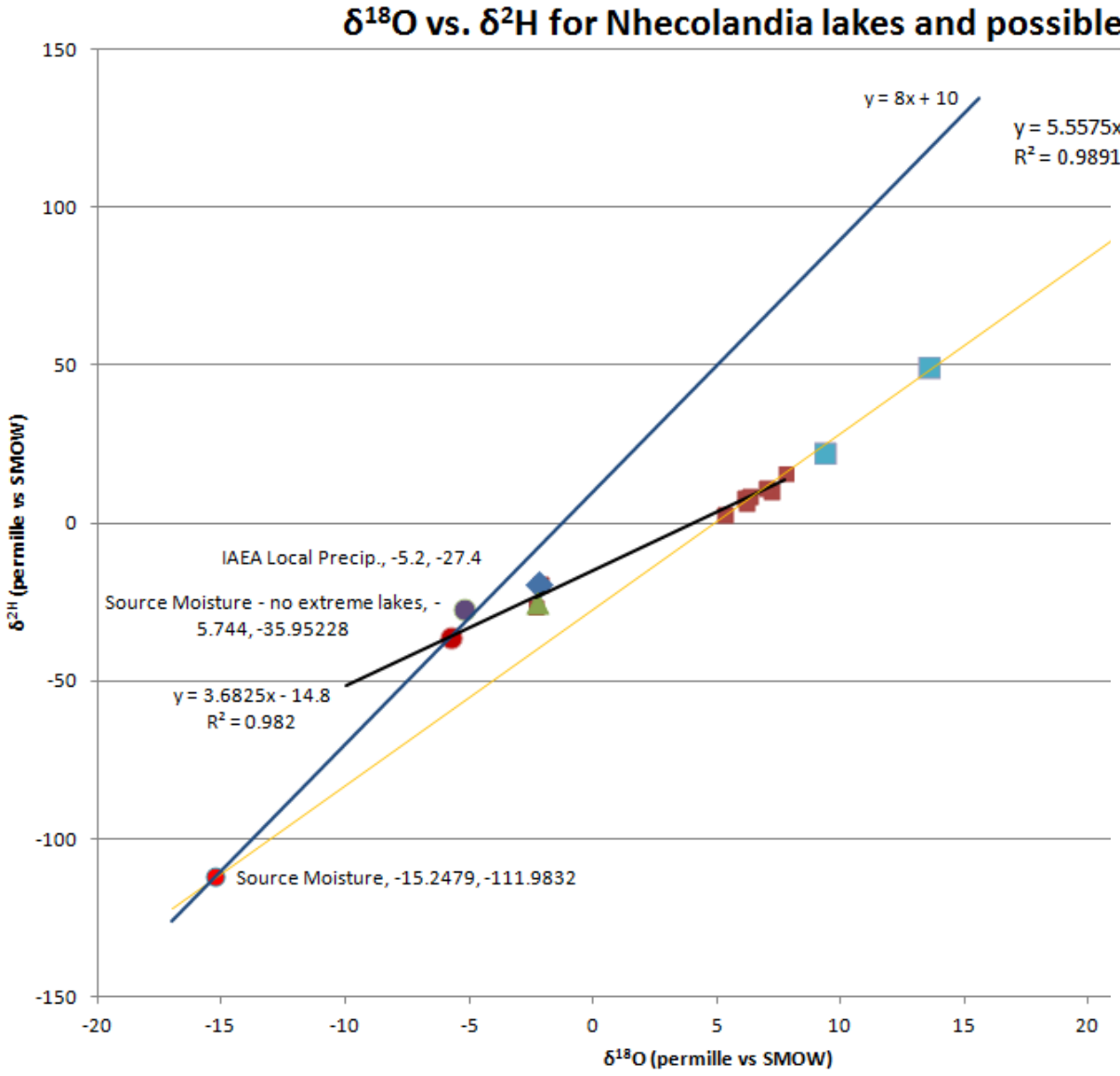

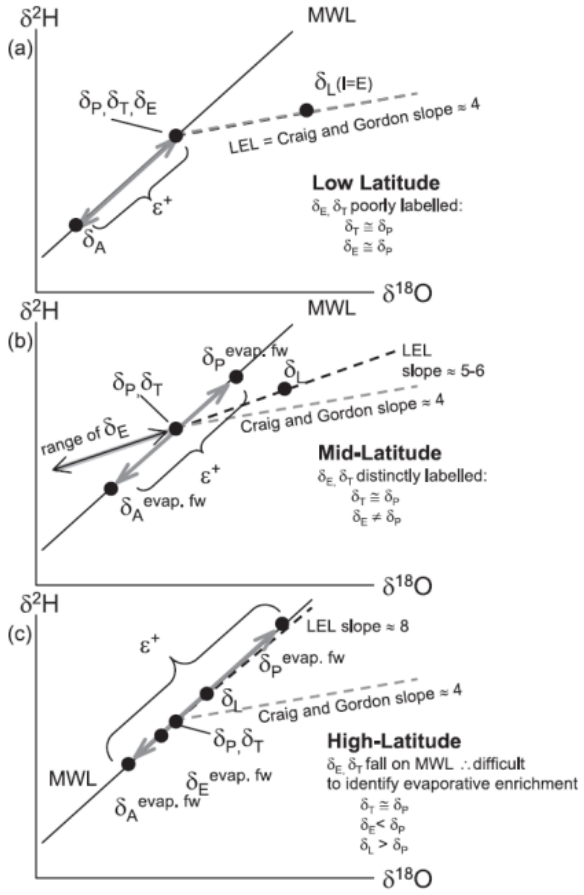

Ribeiro de Almeida, et al. (2010)

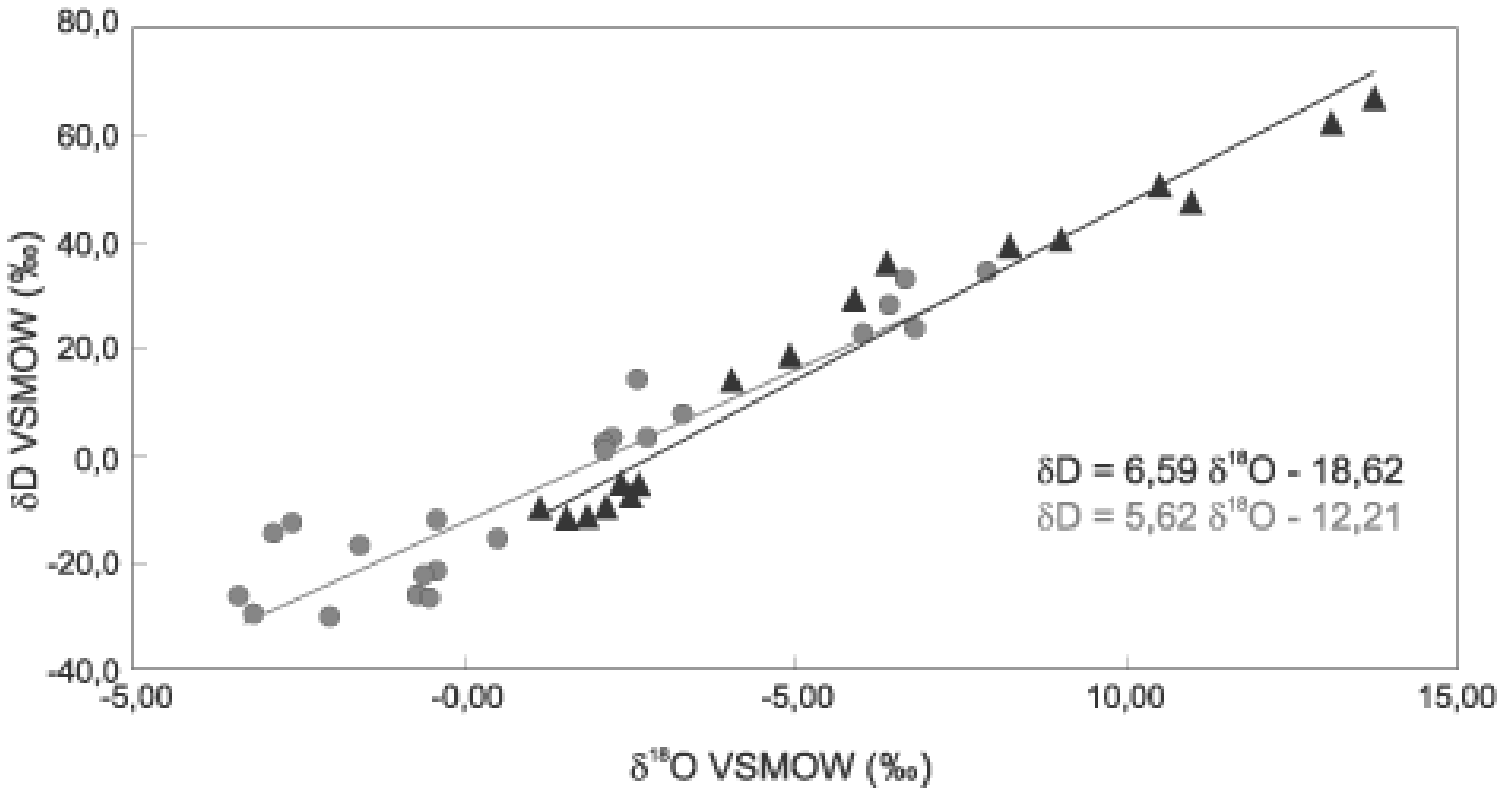

Figura 4. Diagrama de δD x $\delta^{18}O$ do conjunto de amostras da pesquisa, separadas em baixa a média salinidade (círculos em cinza claro) e alta salinidade (triângulos em cinza escuro). Observar a tendência de maior enriquecimento relativo em Deutério para as águas de maior salinidade, indicando maior ação da evaporação e separando os lagos em dois conjuntos em relação ao isolamento dos corpos d'água.

Cl- vs. deltaD

Tabela 4. Médias por classes de água (como Tabela 1) de todos os dados obtidos de Condutividade elétrica (µS.cm^{-1}), Cl^- (mg.L^{-1}); δD SMOW (‰) e $\delta^{18}O$ SMOW (‰) (**n**=número de análises para isótopos; **n^1**=número de dados de Condutividade elétrica e Cl^-.

Classes de água	Condutividade elétrica µS.cm^{-1}	Cl^- (mg.L^{-1})	δD (SMOW)	$\delta^{18}O$ (SMOW)
Água doce (n = 11; n^1 = 13)	52,7	5,35	-6,5	1,4
Baixa a média salinidade (n = 11; n^1 = 13)	288	12,3	3,49	3,01
Alta salinidade (n = 9; n^1 = 9)	1320	81,9	-2,26	2,8
Muito alta salinidade (n = 13; n^1 = 13)	3244	359	16,5	5,25
Hipersalinas (n = 12; n^1 = 12)	9093	2341	28,1	6,61

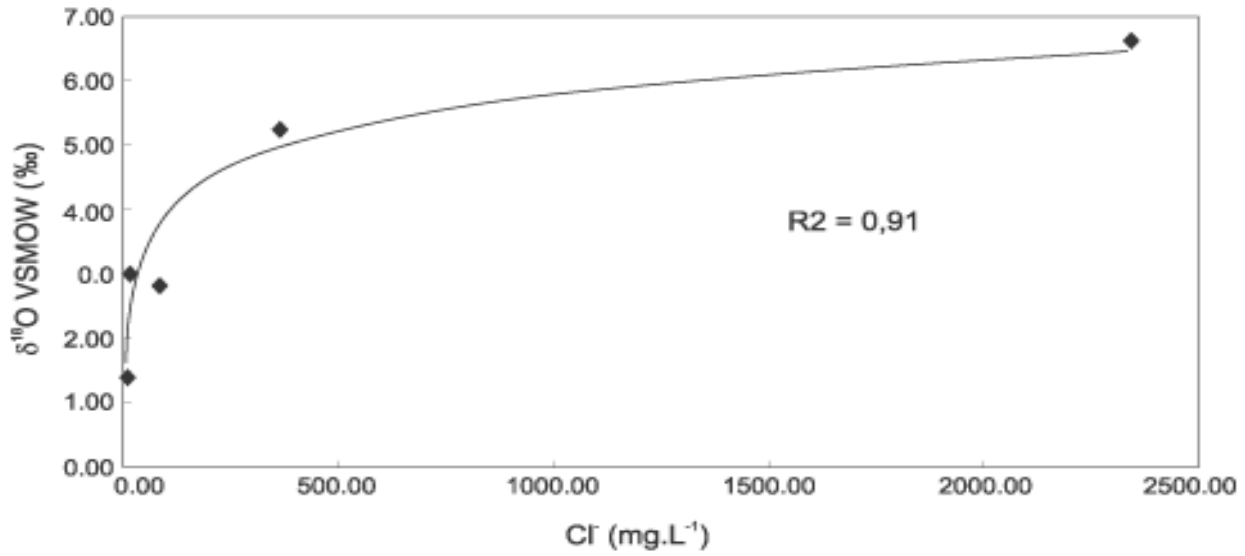

Figura 6. Diagrama Cl^- (mg.L^{-1}) x $\delta^{18}O$ (SMOW) mostrando correlação logarítimica entre o aumento da salinidade e da presença de ^{18}O na água líquida em função da evaporação.

- From Ribeiro de Almeida et al., 2010

ID	Ca	Mg	Na	K	Na + K	HCO3	SO4	Cl	TDS	Balance	0	D	avg Cl	avg D
Rio	1.464	0.924	1.259	2.441	3.7	15.46781	0.481484	1.110273	26.84757	-5.10	-2.16776	-19.3243	2.719313	-8.07344
L20	0.326	0.294	4.094	8.739	12.833	24.7485	0.520061	4.328353	55.88291	-9.85	5.267566	3.177405		
L27	5.688	4.924	55.08	19.204	74.284	228.9236	0.320313	7.03549	395.4594	-5.07	6.299983	8.819034		
L19	3.57	2.56	171.925	60.46	232.385	612.5253	5	17.92828	1106.354	-5.68	6.194585	6.609285		
L10	7.807	1.378	252	80.82	332.82	791.9518	13.76022	37.95213	1518.489	-2.90	6.070025	8.068787	20.97197	7.832369
L11	2.53	0.24	843.2	163.92	1007.12	2091.248	20	382.3613	4510.619	-4.71	6.980277	11.35577		
L29	2.51	3	963.2	179.96	1143.16	2369.668	22.85516	231.6018	4915.955	0.83	9.360107	22.46076		
L22	0.59	3	1181.2	168.24	1349.44	2604.779	20	365.4459	5692.695	2.48	7.76477	15.86392	326.4697	16.56015
L26	3	3	3084.333	599.4667	3683.8	1781.892	20	4732.769	13908.26	-4.23	7.15035	10.38817		
L25	4.987	0.845	242.1	174.7	416.8	983.7527	0.588634	20.7366	1844.51	-4.39	13.54128	49.46965	2376.753	29.92891

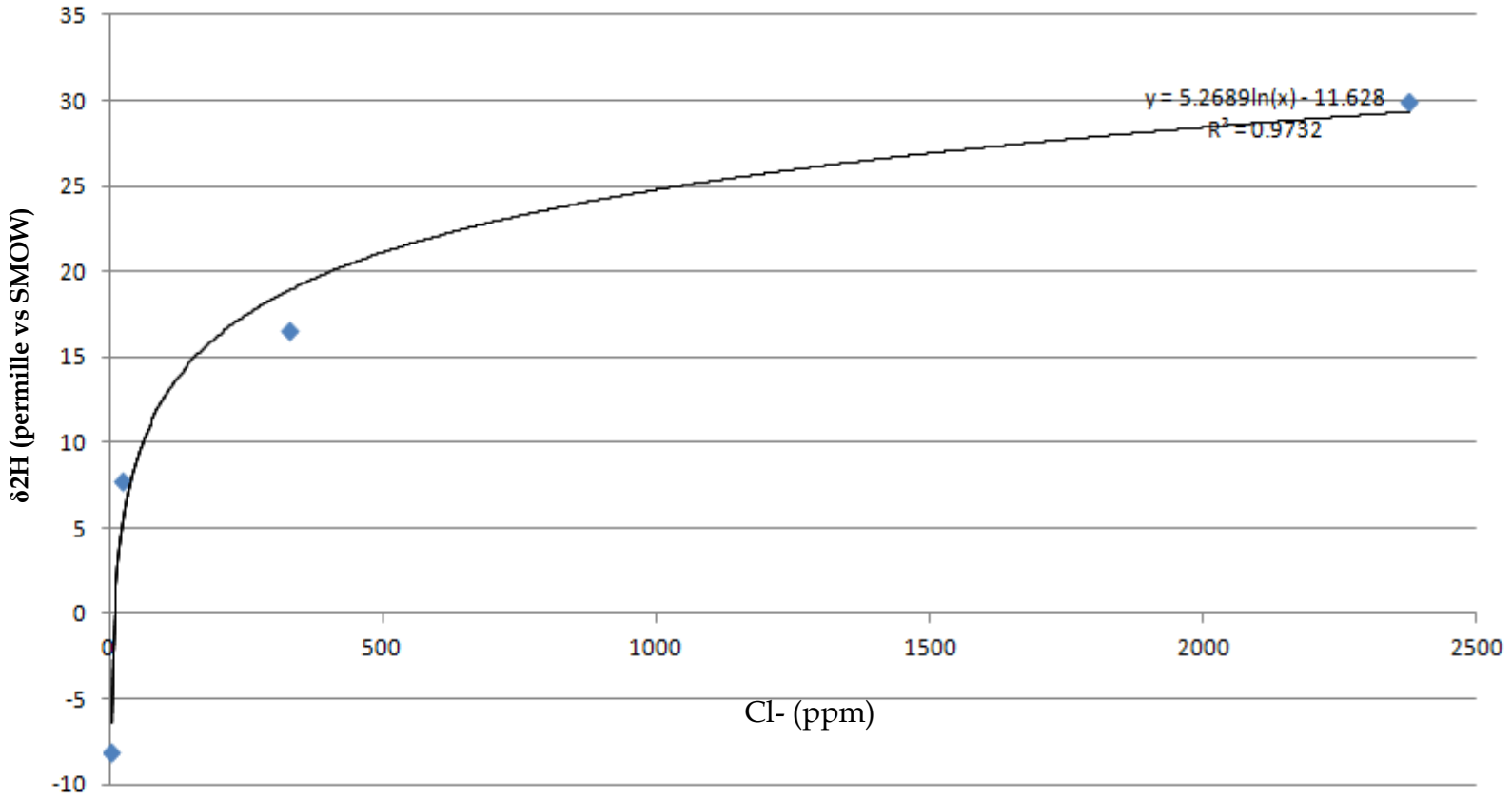

Interpreting anomolies

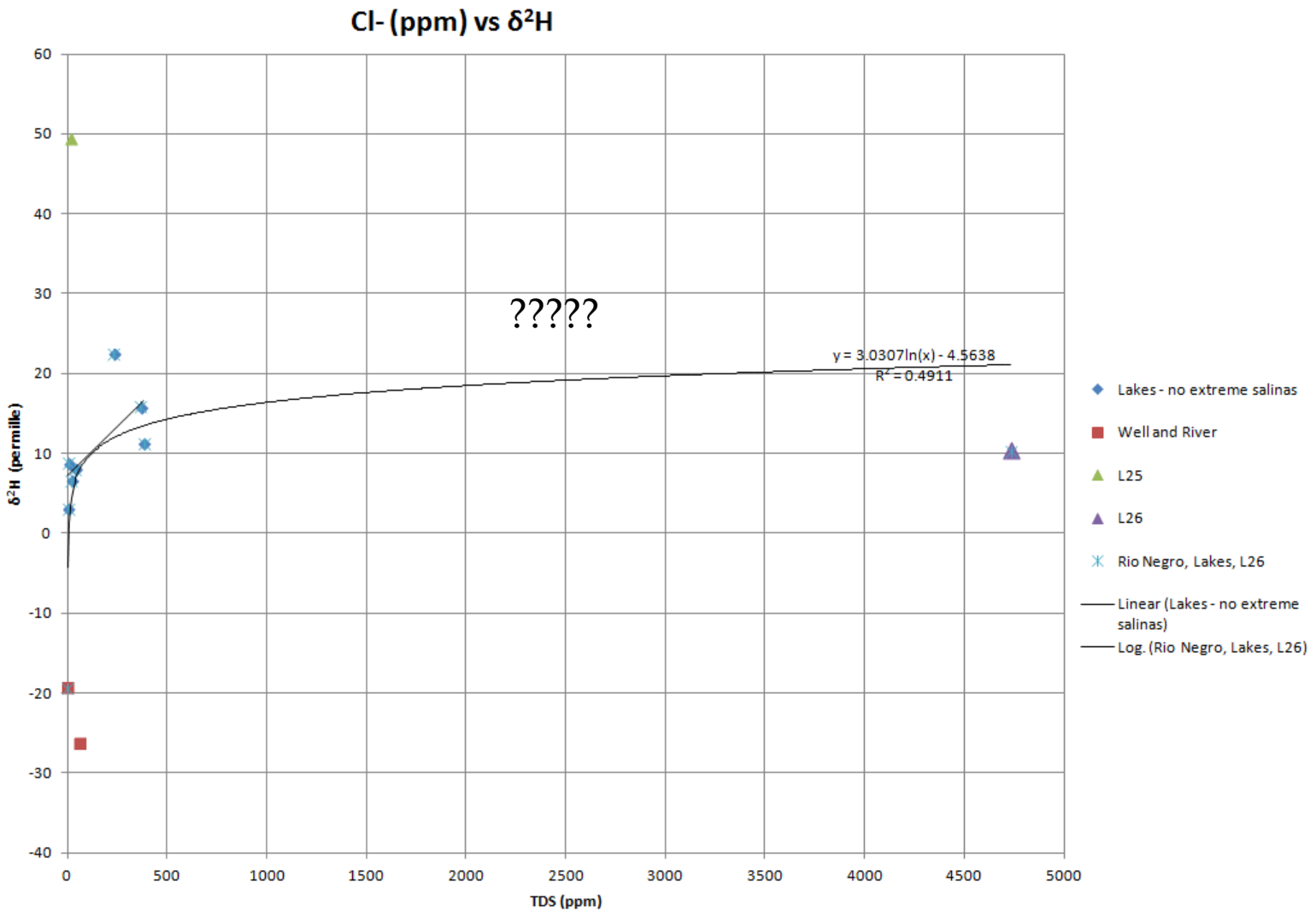

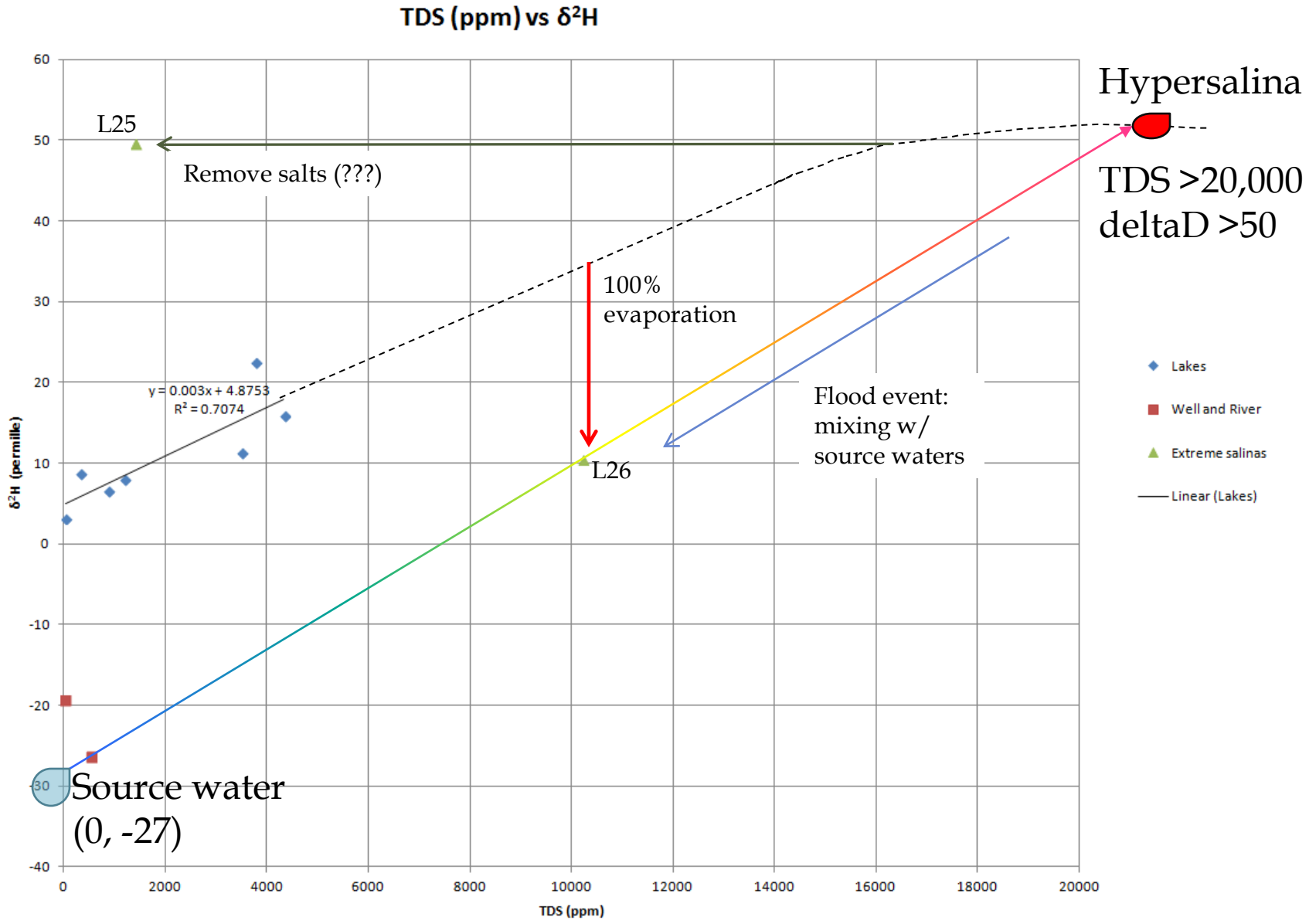
TDS (ppm) vs δ²H
δ²H (permille)
TDS (ppm)
y = 0.003x + 4.8753
R² = 0.7074
L25
Remove salts (???)
100% evaporation
L26
Flood event: mixing w/ source waters
Hypersalina
TDS >20,000
deltaD >50
Source water
(0, -27)
Lakes
Well and River
Extreme salinas
Linear (Lakes)

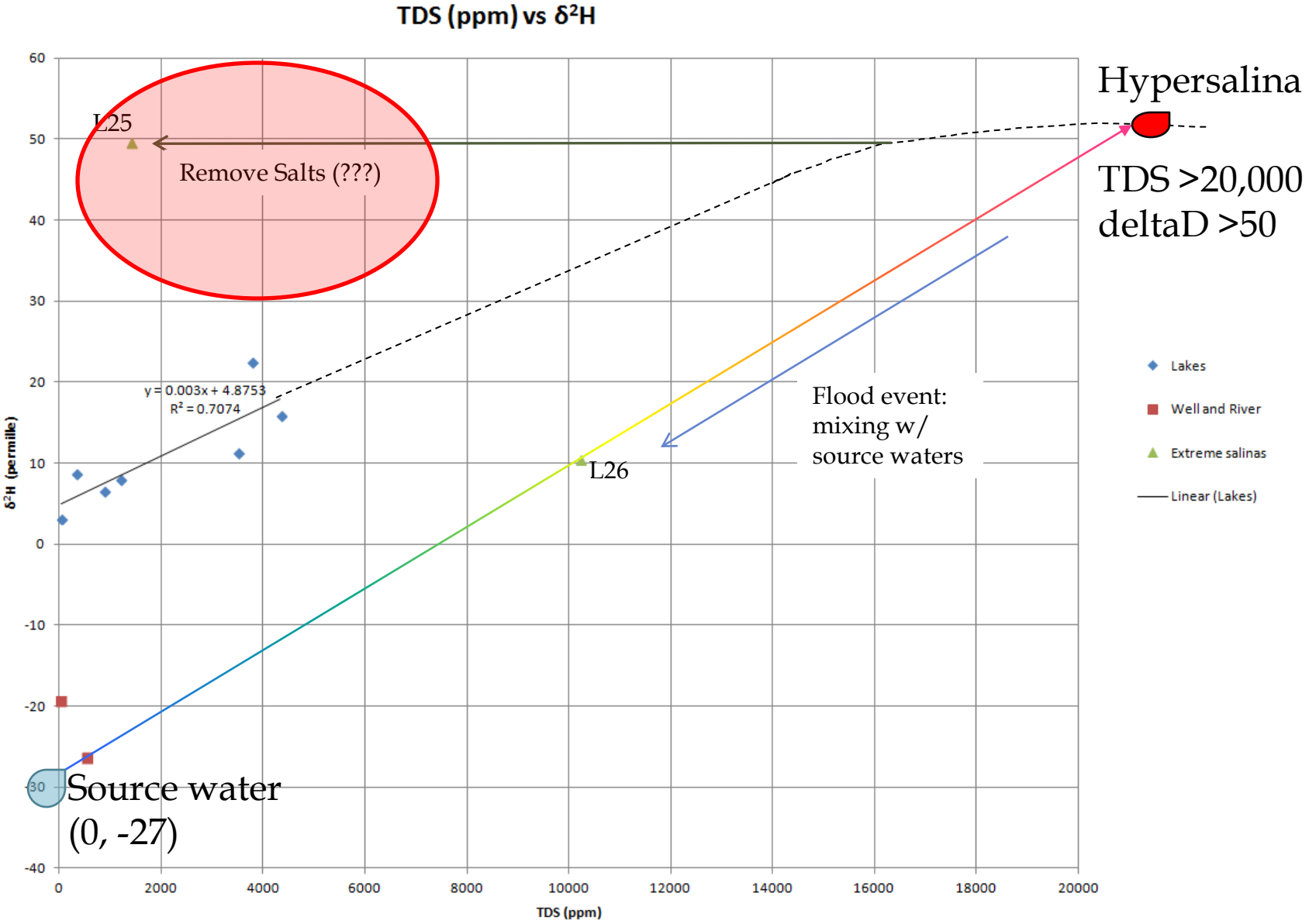
TDS (ppm) vs δ²H
L25
Remove Salts (???)
Hypersalina
TDS >20,000
deltaD >50
y = 0.003x + 4.8753
R² = 0.7074
Flood event:
mixing w/
source waters
L26
Source water
(0, -27)
Lakes
Well and River
Extreme salinas
Linear (Lakes)
δ²H (permille)
TDS (ppm)
60
50
40
30
20
10
0
-10
-20
-30
-40
0
2000
4000
6000
8000
10000
12000
14000
16000
18000
20000

Low lake level
Large mudflat exposed

Impervious green/black layer at ~5 cm

Salty surface crust

Weakly indurated/low permeability if dry

Precipitation of smectites (reducing environment)

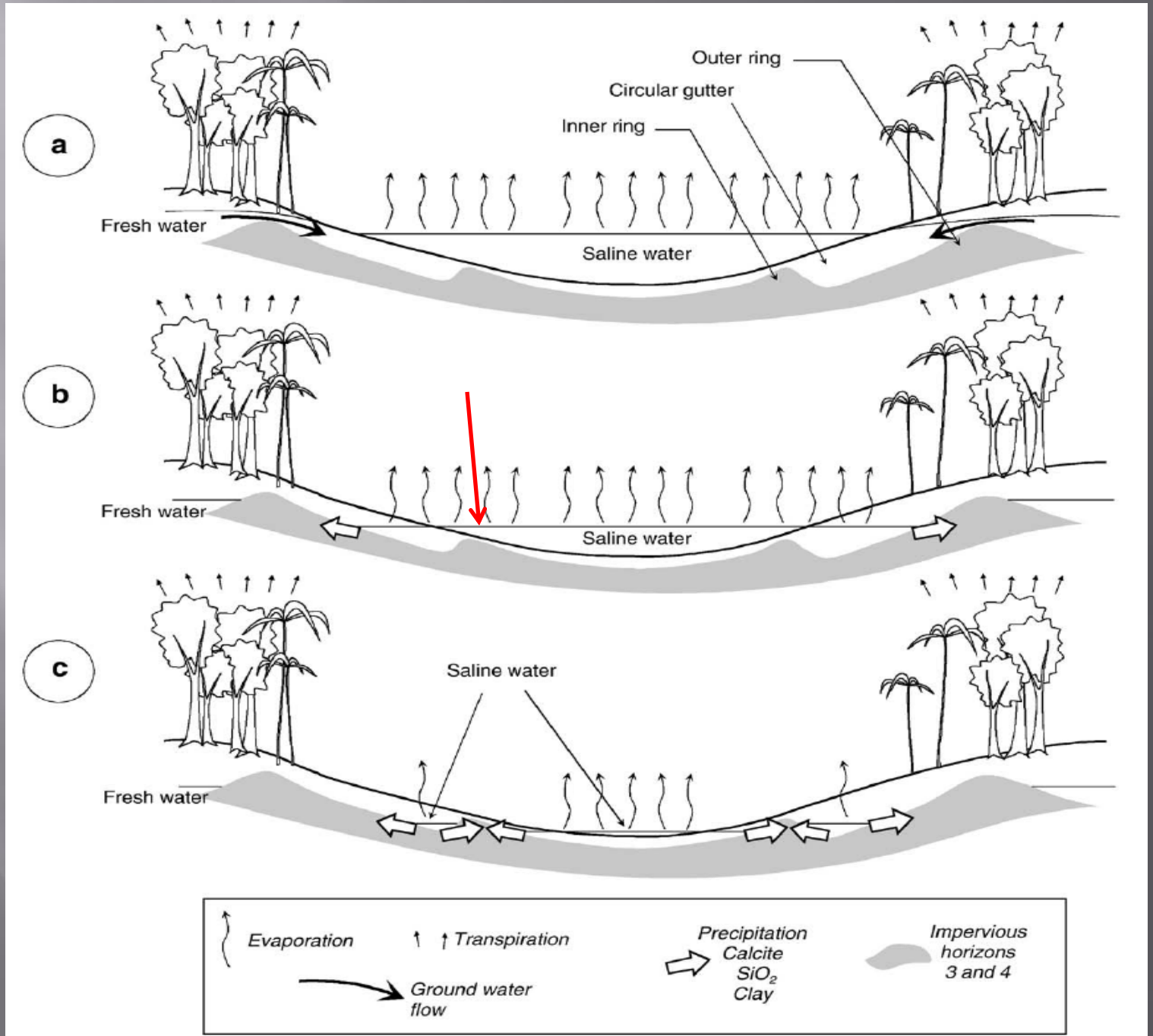
a
Outer ring
Circular gutter
Inner ring
Fresh water
Saline water
b
Fresh water
Saline water
c
Saline water
Fresh water
Evaporation
Transpiration
Ground water flow
Precipitation
Calcite
SiO2
Clay
Impervious horizons 3 and 4

Fate of Salinas?

Oxidation and production of fertile soils?

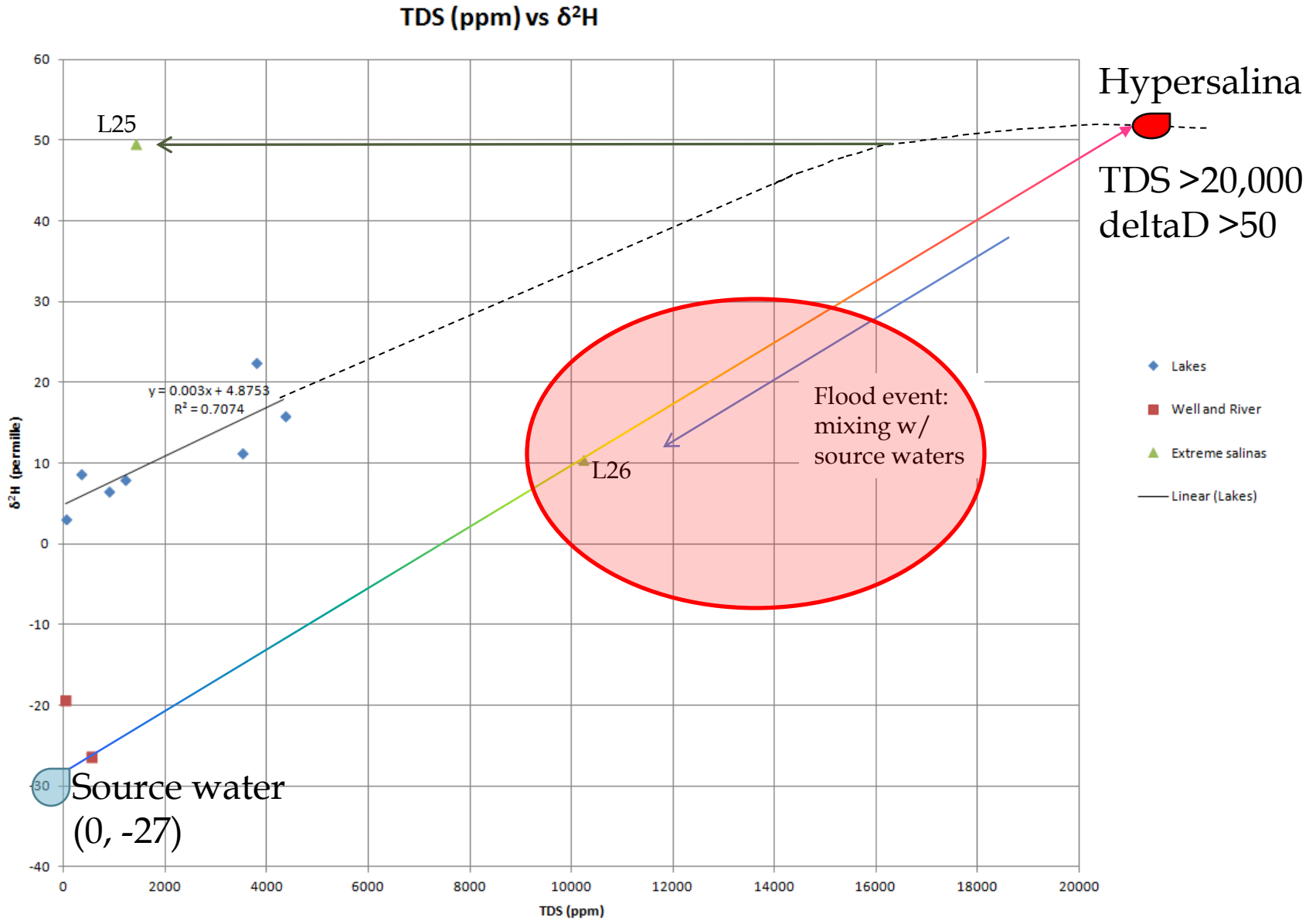
TDS (ppm) vs δ²H
L25
Hypersalina
TDS >20,000
deltaD >50
y = 0.003x + 4.8753
R² = 0.7074
Flood event:
mixing w/
source waters
L26
Source water
(0, -27)
Lakes
Well and River
Extreme salinas
Linear (Lakes)
δ²H (permille)
TDS (ppm)
60
50
40
30
20
10
0
-10
-20
-30
-40
0
2000
4000
6000
8000
10000
12000
14000
16000
18000
20000


High lake level
Water at sandy
“beachline”

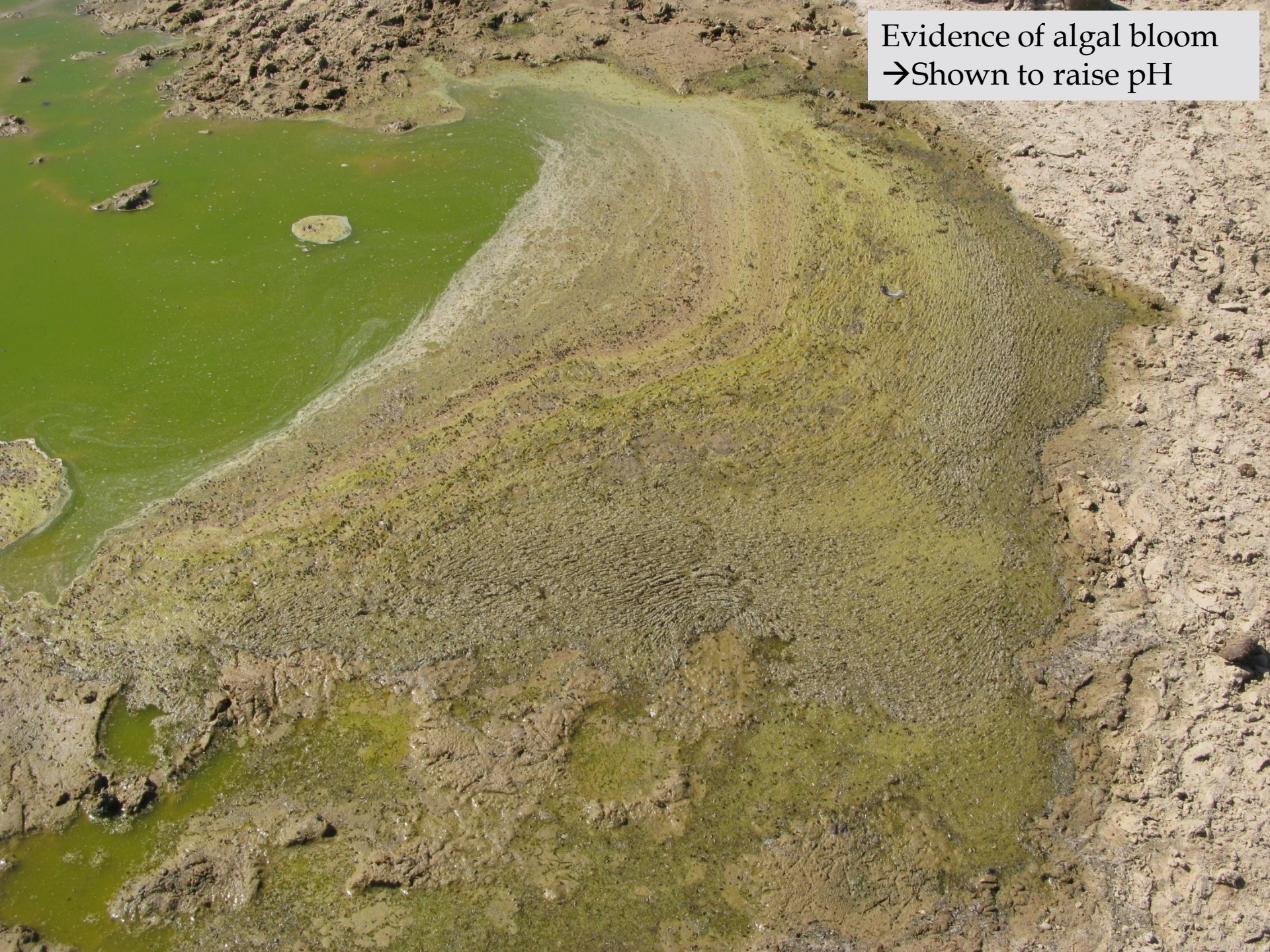
Evidence of algal bloom
→Shown to raise pH

•Evolved from a hypersalina (as L25)
•Crossed chemical divide
•pH > solubility of amorphous Si

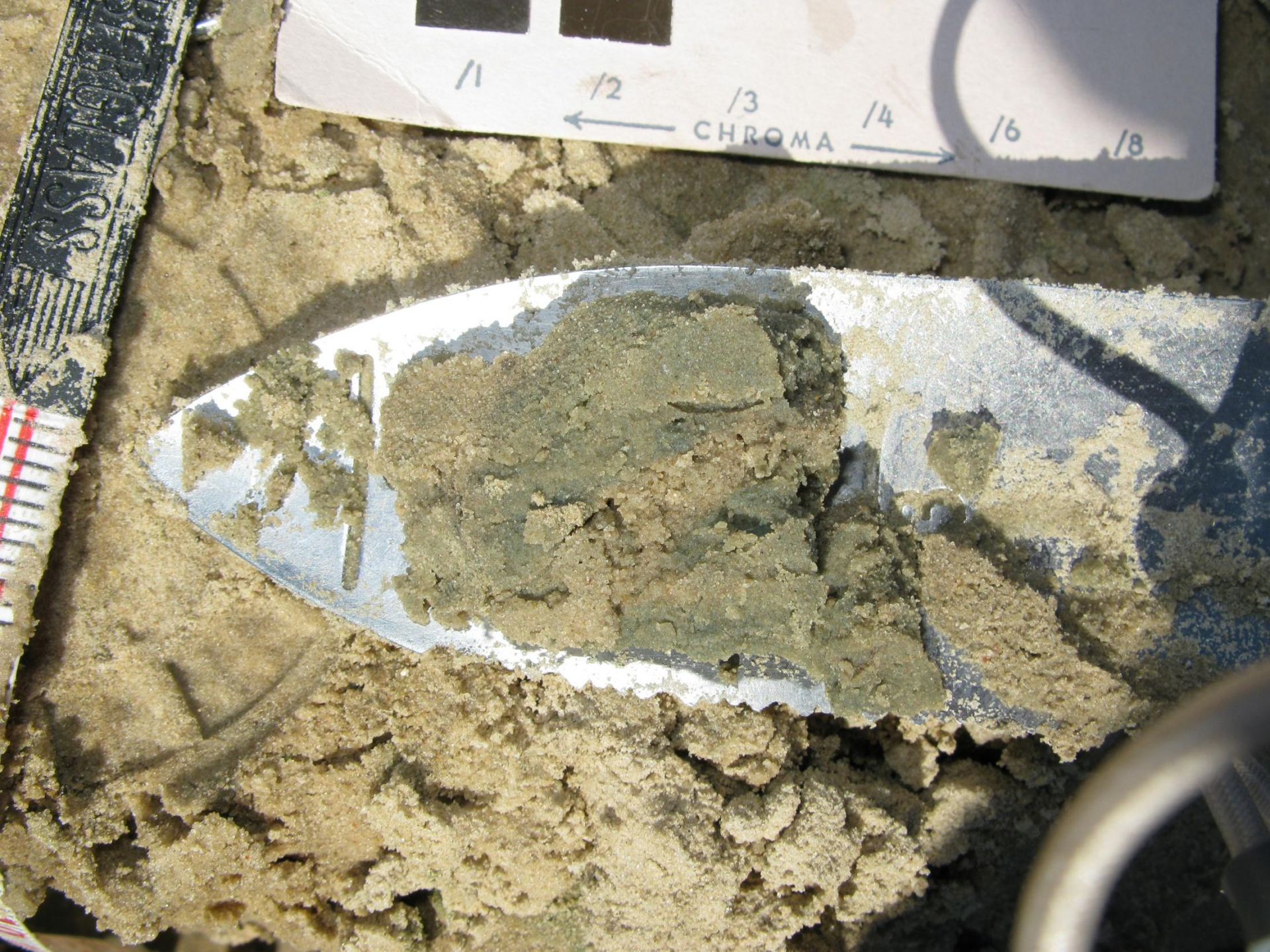
/1
/2
/3
/4
/6
/8
CHROMA


30
40
50
60
70
80
90

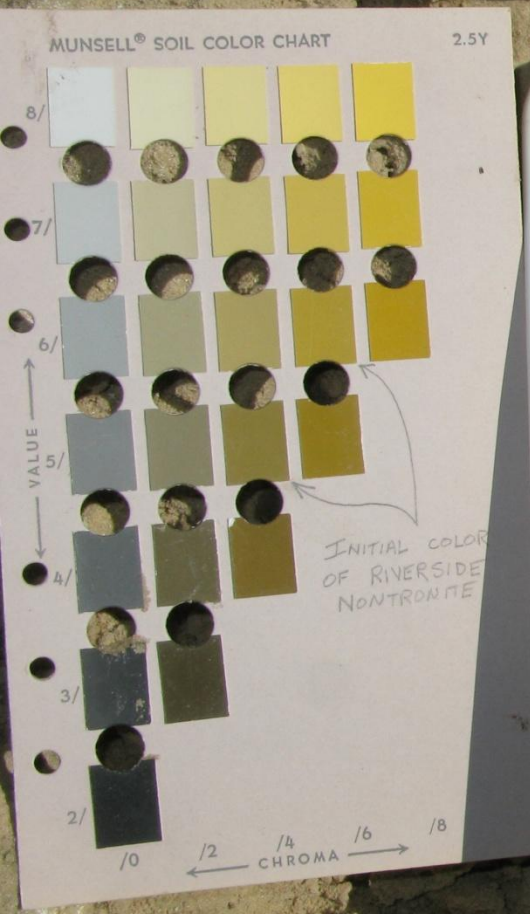

LAKE 11 pH 12 EC
7/23/2012 1:00 pm
Boring & Pit #1
Depth: 120 to 150 cm
Color: 2.5Y 4/2
Texture: SL

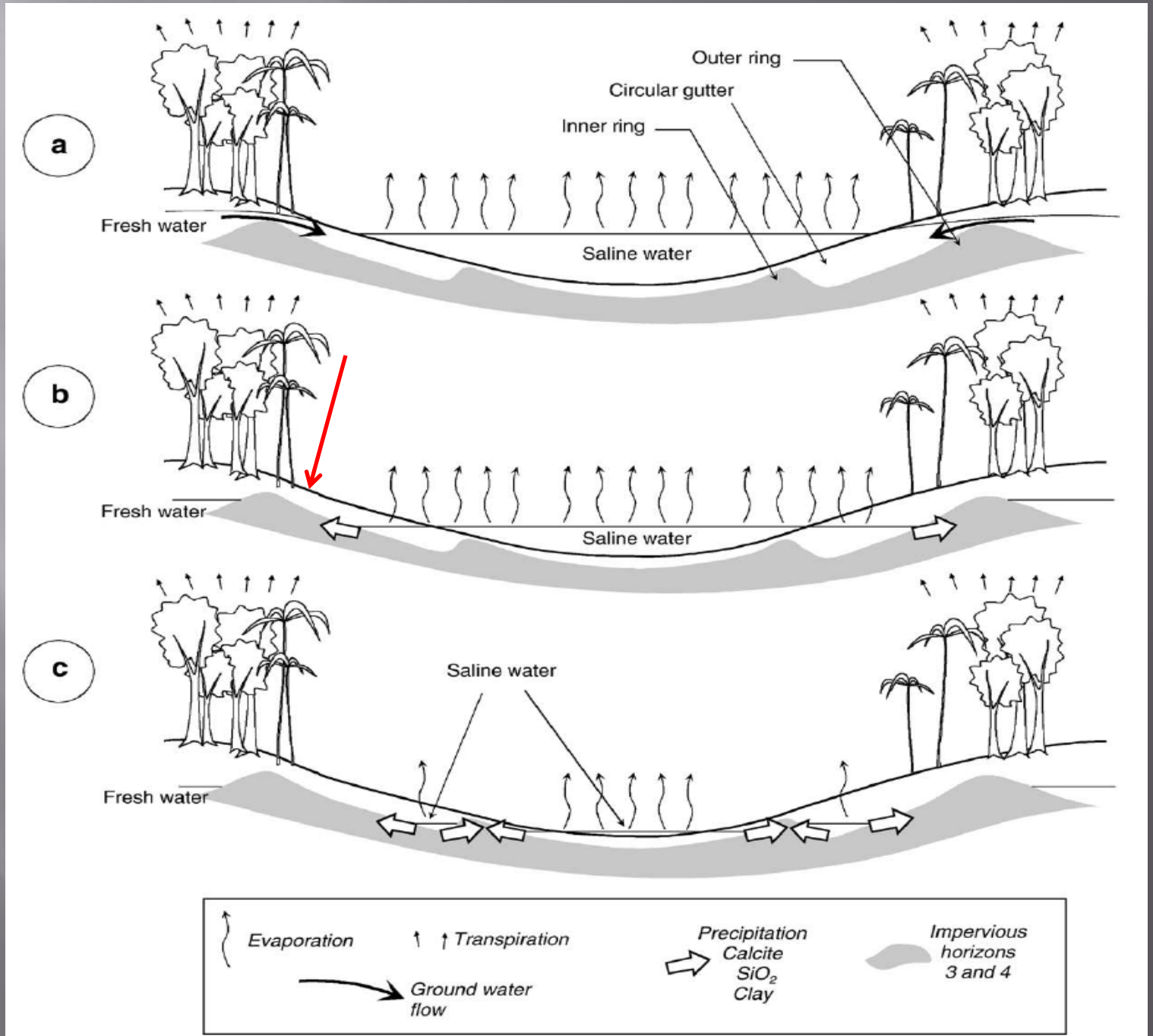
a
Outer ring
Circular gutter
Inner ring
Fresh water
Saline water
b
Fresh water
Saline water
c
Saline water
Fresh water
Evaporation
Transpiration
Ground water flow
Precipitation
Calcite
SiO_2
Clay
Impervious horizons 3 and 4

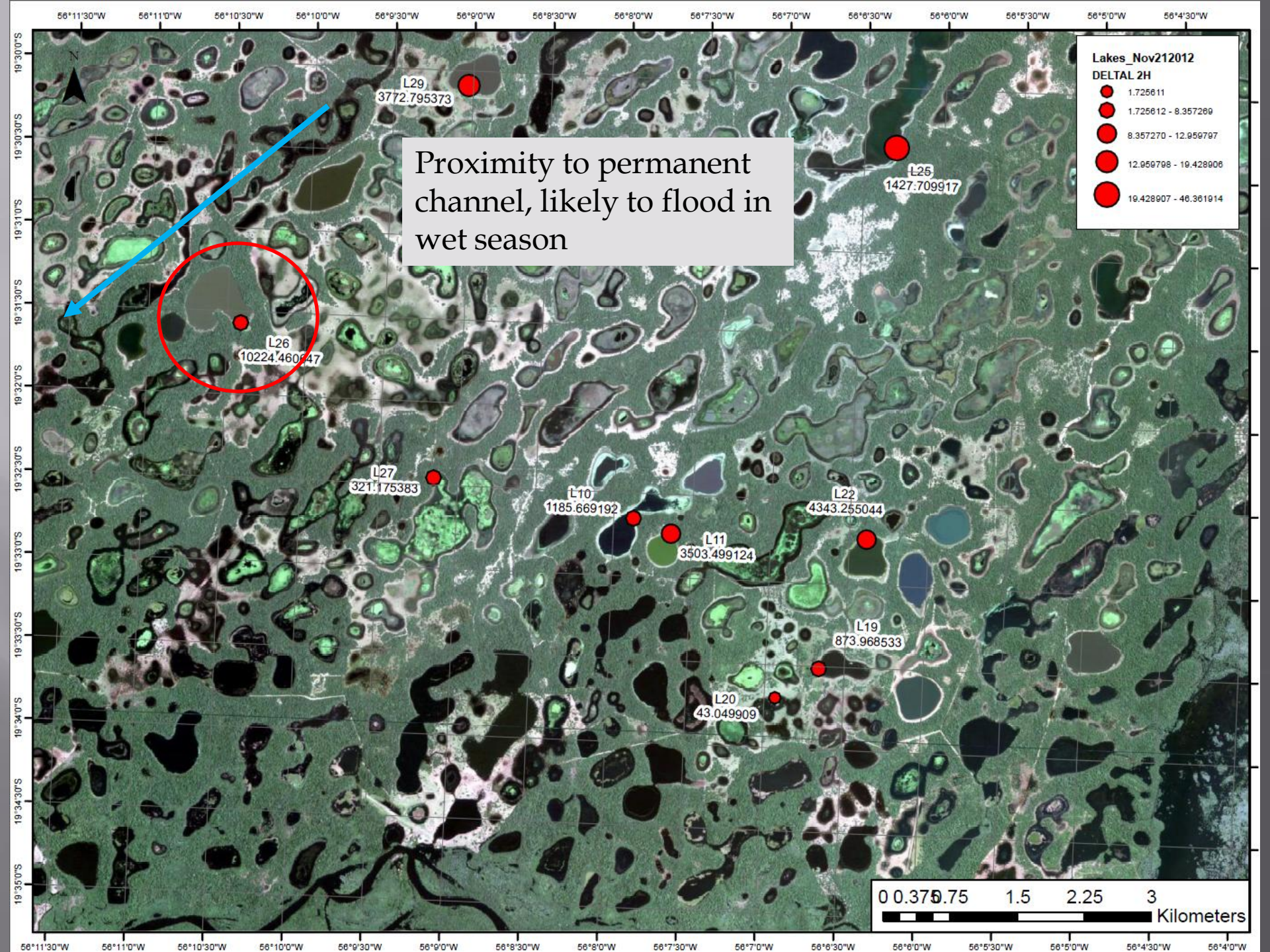
Proximity to permanent channel, likely to flood in wet season
Lakes_Nov212012
DELTAL 2H
1.725611
1.725612 - 8.357269
8.357270 - 12.959797
12.959798 - 19.428906
19.428907 - 46.361914
L29
3772.795373
L25
1427.709917
L26
10224.460647
L27
321.175383
L10
1185.669192
L22
4343.255044
L11
3503.499124
L19
873.968533
L20
43.049909
0 0.375 0.75 1.5 2.25 3
Kilometers
56°11'30"W
56°11'0"W
56°10'30"W
56°10'0"W
56°9'30"W
56°9'0"W
56°8'30"W
56°8'0"W
56°7'30"W
56°7'0"W
56°6'30"W
56°6'0"W
56°5'30"W
56°5'0"W
56°4'30"W
19°30'0"S
19°30'30"S
19°31'0"S
19°31'30"S
19°32'0"S
19°32'30"S
19°33'0"S
19°33'30"S
19°34'0"S
19°34'30"S
19°35'0"S

Site-specific Model: Salinas isolated from GW

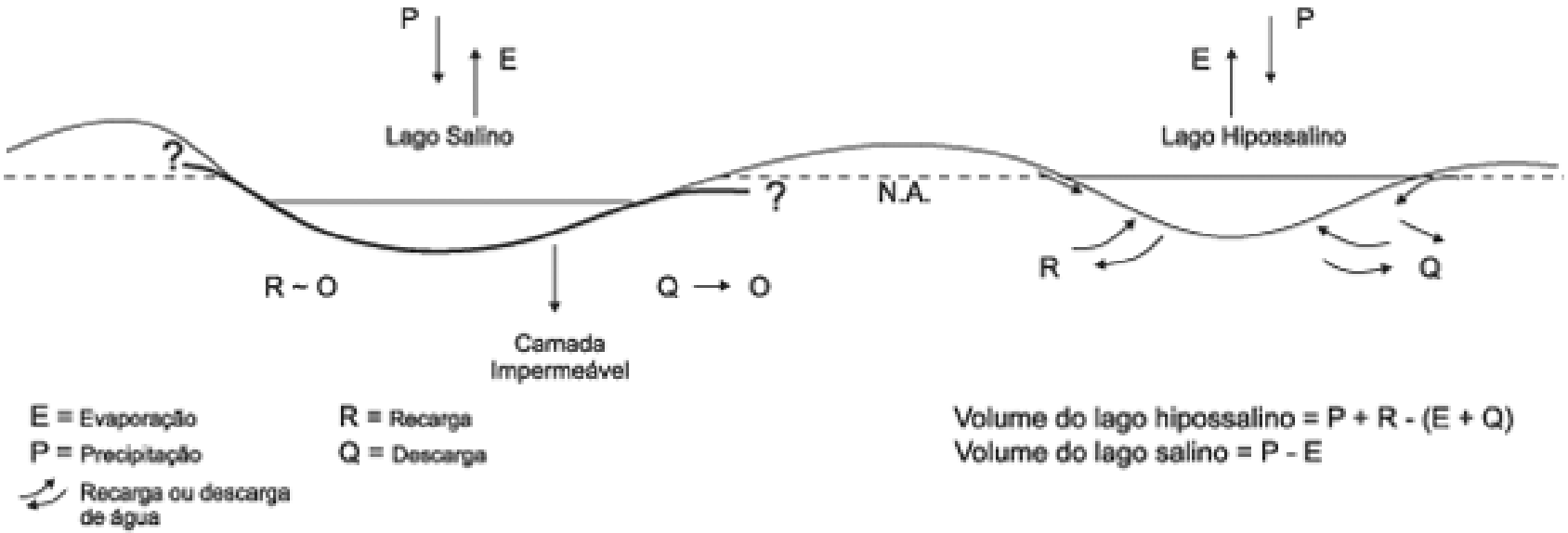

Figura 7. Modelo esquemático das relações dos lagos salinos e hipossalinos da Nhecolândia com o freático.

- From Ribeiro de Almeida et al., 2010

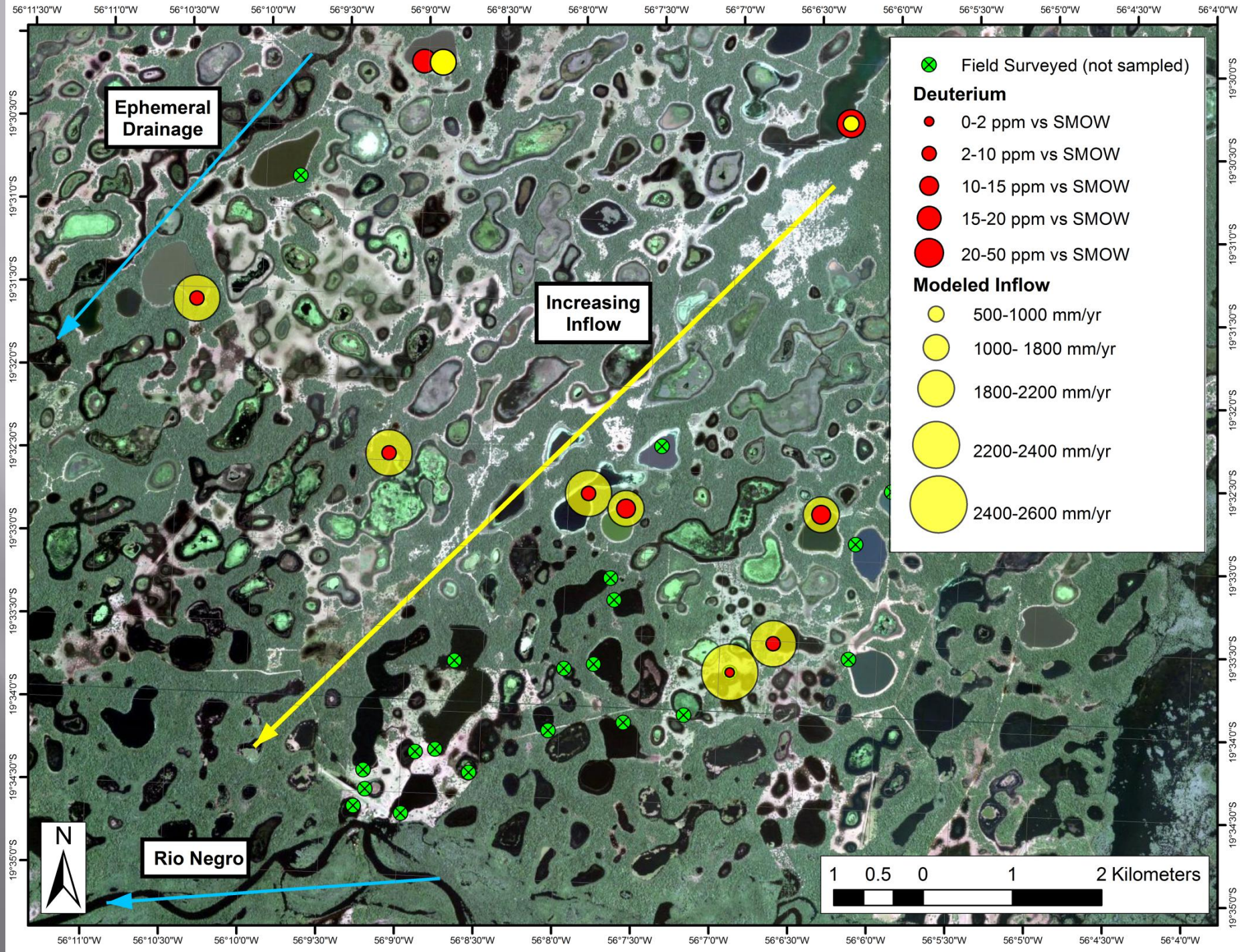
Ephemeral Drainage
Increasing Inflow
Rio Negro
N
Field Surveyed (not sampled)
Deuterium
0-2 ppm vs SMOW
2-10 ppm vs SMOW
10-15 ppm vs SMOW
15-20 ppm vs SMOW
20-50 ppm vs SMOW
Modeled Inflow
500-1000 mm/yr
1000- 1800 mm/yr
1800-2200 mm/yr
2200-2400 mm/yr
2400-2600 mm/yr
1 0.5 0 1 2 Kilometers
56°11'30"W
56°11'0"W
56°10'30"W
56°10'0"W
56°9'30"W
56°9'0"W
56°8'30"W
56°8'0"W
56°7'30"W
56°7'0"W
56°6'30"W
56°6'0"W
56°5'30"W
56°5'0"W
56°4'30"W
56°4'0"W
19°30'30"S
19°31'0"S
19°31'30"S
19°32'0"S
19°32'30"S
19°33'0"S
19°33'30"S
19°34'0"S
19°34'30"S
19°35'0"S

References cited:

Almeida, F.F.M. and Lima, M.A., 1956. Excursion Guidebook 1. 18th International Geography Conges: Rio De Janeiro, Brasil.

Assine, Mario Luis; Silva, Aguinaldo, 2009. Contrasting fluvial styles of the Paraguay River in the northwestern border of the Pantanal Wetland, Brazil. Geomorphology v113, 3-4,p.189-199.

Assine, M. L., 2005. River avulsions on the Taquari megafan, Pantanal wetland, brazil. *Geomorphology, 70*(3-4), 357-371.

Assine, M.L., Soares, P.C., 2004, Quaternary of the Pantanal, west-central Brazil: Quaternary International, v 114, p. 23-34.

Barbeiro, L., Filho, A.R., Furquim, S., Furian, S., Sakamoto, A.Y., Valles, V., Graham, R.C., Fort, M., Ferreira, R., Neto, J., 2008. Soil morphological control on saline and freshwater lake hydrogeochemistry in the Pantanal of Nhecolandia, Brazil. Geoderma, v. 148(1), p. 91-106.

Barbeiro, L., Graham, R.C., Furian, S., 2010. Neoformation of micas in soils surrounding an alkaline-saline lake of Pantanal wetland, Brazil. Geoderma, v. 158(3-4), p. 331-42.

Barbeiro, L., Queiroz Neto, J.P., Ciornei, G., Sakamoto, A.Y., Capellari, B., Fernandes, E., Valles, V., 2002. Geochemistry of water and groundwater in the Pantanal. Wetlands, v. 22(3), p. 528-540.

Bertani, T.C., Novack, T. Hawyawaka, E.H., Zani, H., 2007, Detection of saline and non-saline lakes on the Pantanal of Nhecolandia (Brazil) using object-based image analysis. Internatiional Archives of the Photogrammetry, Remote Sensing, and Spatial Information Sciences, v. 38(4)/C7.

Buehler, H.A, Weissmann, G.S., Scuderi, L.A., and Hartley, A.J., 2011 Spatial and Temporal evolution of an avulsion on the Taquari River distributive fluvial System from satellite image analysis. Journal of Sedimentary Research, p. 630-640.

Colinvaux, P.A., Oliveira, P.E., Bush, M.B., 2000. Amazonian and neotropical plant communities on glacial time-scales: the failure of the aridity and refuge hypothesis. Quaternary Science Reviews, v. 19, p. 141-169.

Gradella, F., Zani, H., Silva, A., Kuerten, S., Corradini, F.A., Sakamoto, A.Y., 2011, geomorphology and deposition events in Nhecolandia, Pantanal wetland: Geografia (Rio Claro), v. 3, p. 107-117.

Ellwein, A.L., Mahan, S.A., McFadden, L.D., 2011 (in press). New optically stimulated luminescence ages provided evidence of MIS3 and MIS2 eolian activity on Black Mesa, northeastern Arizona, USA. Quaternary Research (in press).

Fernandes, E., Sakamoto, A.Y., Queiroz Neto, J.P., Lucati, H.M., Capellari, B., 1999. Le Pantanal da Nhecolandia Mato Grosso: Cadre physique et dynamique hydrologique. Geografica Fisica e Dinamica Quaternaria, . 22, p. 13-21.

Furquim, S., Graham R.C., Barbiero, L., Neto, J., Valles, V., 2008. Mineralogy and genesis of smectites in an alkaline saline environment of Pantanal wetland, Brazil. Clays and Clay Mineralogy, v. 56(5), p. 579-95.

Furquim, S., Graham, R.C., Barbiero, L., Neto, J., Vidal-Torrado, P., 2010. Soil mineral genesis and distribution in a saline lake landscape of the Pantanal wetland, Brazil. Geoderma, v. 154(3-4), p. 518-28.

Furquim, S., Barbiero, L., Graham, R.C., Queiroz Neto, J.P., Dias Ferreira, R.P., Furian, S., 2010. Neoformation of micas in soils surrounding an alkiali-saline lake of Pantanal wetland, Brazil. Geoderma, v. 158, p. 331-342

Hartley, A.J., Weissmann, G.S., Nichols, G.J., Warwick, G.L., 2010. Large distributive fluvial systems: Characteristics, distribution, and controls on development. Journal of Sedimentary Research, v. 80(2).

Klammer, G., 1982, The paleodesert of Pantanal and the Pleistocene climate history of tropical regions: Zeitschrift fur Geomorphologie, v. 26(4), p.393.

Martins, E.R., Furian Dias, S.M., Barbeiro, L., Parizzot, T.M., Filho, A.T., *in press*. Spatial chemical variability of surface water in the Nhecolandia, Pantanal (MS), Brazil. Web available (April 2012):
http://acreditacion.fisa.cl/ugi/contenidos/ponencia/38/CurtiMartinsElis%E2ngelaRosemeri_201115688FZ5EA_f.doc

Mourao, G.M., Ishii, T.H., Campos, Z.M.S, 1988. Alguns factores limnologicos relacionados com a ichtiofauna de lagoas e *salina*s do pantanao da Nhecolandia, MS, Brasil. Acta Limnologica Brasiliensia , p. 181-198.

Ribeiro de Almeida, T.I., Sigolo, J.B., Fernandes, E., Queiroz Neto, J.P., Barbiero, L., Sakamoto, A.Y., 2003. Proposta de clasificacao e genese das lagoas da biaxa Nhecolandia-MS com base em sensoriamento remoto e dados de campo. Revista Brasileira de Geociencias, v 33 (2), p. 83-90.

Soares, A.P., Soares, P.C., Assine, M.L., 2003, Areiais e lagoas do Pntanal: Heranca paleoclimatica? Revista Brasilieira de Geociencias, v. 33(2), p. 211.

Tricart, J., 1982, El Pantanal: Un Ejemplo del impacto de la Geomorfoloiga sobre el medio ambiente. Geografia, v. 7(13-14), p. 37-50.

Ussami, N., Shiraiwa, S., Landim, Dominguez, J.M., 1999,Basement reactivation in a sub-Andean foreland flexural bulge: The Pantanal wetland, SW Brazil: Tectonics, v. 18, no.1, p. 25-39.

Whitney, B.S., Mayle, F.E., Punyasena, S.W., Fitrzpatrick, K.A., Burn, M.J., Guillen, R., Chavez, E., Mann, D., Pennington, R.T., Metcalfe, S.E., 2011. A 45 kyr palaeoclimate record from the lowland interior of tropical South America. Palaeogeography, Palaeoclimatology, Palaeoevology, v. 307, p.177.

Weissmann, G.S., Hartley, A.J., Nichols, G.J., Scuderi, L.A., Olson, M., Buehler, H., Banteah, R. 2010. Fluvial form in modern continental sedimentary basins: Distributive fluvial systems. Geology, v. 38(1), p.39-42.

Zani, H., Assine, M.L., Silva, A., Corradini, F.A., 2009. Redes de drenagem distributaria e formas deposicionais no megaleque do Taquari, Pantanl: Um analise baseado no MDE-SRTM. Revista Brasileira de Gemorfologia, v.10(2), p. 21-27.

Zani, H., Assine, M.L., 2011. Paleocanais no megaleque do Rio Taquari: mapeamento e significado geomorfologico. Revista Brasileira de Geoceincias, v. 41(1), p. 37-43.

Zani, H., Assine, M.L., 2009, Analise de superficies de tendencia com dados SRTM: estado de caso na bacia sedimentar do Pantanal: Annals XIV of the Brazilian Symposium of Remote Sensing, Natal, Brasil, p. 25-30.

Zani, H., Assine, M.L, Araujo, B.C., Merino, E.R., Silva, A., Fanciani, E.M., 2006. Lobos deposicionais na evolucao do megaleque do Rio Taquari, Pantanal Mato-grossense. 1st Annals of Geotechnolocy in the Pantanal: Campo Grande, Brasil (INPE), p. 285-292.